INVESTIGATION OF THE FRICTION AND NOISE OF AUTOMOTIVE RUBBER BELT

By

Vikram R. Narravula

RECOMMENDED: _____

_____

_____

Advisory Committee Chair

_____

Chair, Department of Mechanical Engineering

APPROVED: _____

Dean, College of Engineering and Mines

_____

Dean of the Graduate School

_____

Date

INVESTIGATION OF THE FRICTION AND NOISE OF AUTOMOTIVE RUBBER BELT

A

THESIS

Presented to the Faculty

of the University of Alaska Fairbanks

in Partial Fulfillment of the Requirements

for the Degree of

MASTER OF SCIENCE

By

Vikram R. Narravula, B.E.

Fairbanks, Alaska

May 2011

ABSTRACT

The objective of this research was to study the frictional properties of an automotive v-ribbed belt-pulley system. In order to evaluate the friction and noise, a new test setup was constructed. The assembly was run under various environmental and operational conditions and the results were quantifed, studied, and compared among themselves. The environmental conditions included dry interface and wet interface, conducted at both room temperature (23^{o}C) and cold temperature (-20^{o}C). Operational parameters varied during the experiment were wrap angle, load attached, and acceleration. Frictional forces and associated noises generated were recorded. Some of the results generated were compared with previous reseach work, and the setup was also used to generate new data for conditions not previously studied. Dry room temperature results show close corelation with previous research. The presence of water in liquid state in the interface induces larger adhesion as water film in the interface changes friction mechanisms in the rubber belt-pulley interface. The high stiction of wet friction can lead to stick-slip vibrations and squeal noise. The theoretical stiction model for wet belt-pulley interface is presented. The stiction-related noise test is conducted, and the result is used to identify the spectrum pattern. The belt friction under cold conditions is found to have a higher value than that in room temperature conditions. The belt noise under cold conditions is found to have much higher squeal frequency than that in room temperature conditions.

Table of Contents

Page

Page

Page

List of Figures

Page

Page

Page

List of Tables

Page

ACKNOWLEDGMENTS

I take great pleasure in expressing my heartfelt thanks to my principal advisor, Dr. Gang Sheng (Gang Chen), for his constant support, kindness, encouragement and invaluable guidance during this research. I would also like to thank my advisory committee members, Dr. Jonah Lee and Dr. Cheng-fu Chen, for taking time out of their busy schedules to help me complete my thesis.

For financial support, the Department of Mechanical Engineering and INE are gratefully acknowledged, with special thanks to INE for allowing me to use the cold chamber for part of my cold temperature testing. I would also like to thank the Technical Support Services of the College of Engineering and Mines for allowing me to conduct the rest of my cold experiment testing in the garage.

I remain indebted to Eric Johansen at the Mechanical Department machine shop for all his help in machining certain components of the experimental setup. Undergraduates David Song and Tristan Kitchin helped in building the setup and conducting the experiments. Dr. Rorik Peterson helped me figure out the finer details of the load cell and LabVIEW. Michael Golub allowed me to use the DC motor and the batteries. Dr. Jun Zhang and Dr. Hui Zheng did Finite Element Method analysis and measured the roughness of the belt used. I thank you all for your support.

I remain grateful to my parents, Mr. Dwarakanath Reddy and Mrs. Bhagyalakshmi, and my sister Mrs. Madhuri, on whose constant encouragement and love I have relied throughout my academic life. Finally, I would like to thank my friends for their support and comments about my work.

CHAPTER 1

INTRODUCTION

1.1 Introduction

Start-up or overload torque often causes tangential slippage in the accessory belt. Wet conditions can increase the slippage substantially and cause an easily perceptible noise called wet belt slip noise. Existing experiments show that this kind of easily perceptible noise could occur for some applications under wet slip conditions. This usually occurs abruptly and with a higher sound pressure level even when the system running conditions are changed continuously. The friction of rubber under cold conditions is extremely significant to the safety and performance of vehicles and machines in cold climates. Friction properties of dry rubber have been studied previously; however, they have not been extensively studied at cold temperature. This research studies the start-up friction and noise properties of a v-ribbed belt-pulley system under such conditions. Wet belt slip noise has been observed and reported for many years, but quantification of the noise still remains elusive.

1.2 Review of Research on Rubber Belt-Pulley Friction

The automotive serpentine v-ribbed rubber belt system has been studied by various researchers. Meckstroth and Ahoor [1, 2] studied the tribological and dynamic properties of belts. Connell and Rorrer [3] investigated friction-induced vibration and

noise in v-ribbed belt applications. Dalgarno, Moore, and Day [4] studied tangential slip noise of v-ribbed belts. Sheng et al. [5, 6] investigated friction-induced vibration and noise in v-ribbed belt applications. In their study [5], the noise generation mechanism in v-ribbed belt applications was formulated mathematically. The model was simplified and used to correlate with experimental results.

Sheng et al. [6] conducted a set of experiments using an industry standard test rig and a standard material friction tester. The resulting wet friction and friction-induced slip noise in accessory belt drive systems were quantified and investigated. The experiments showed that in many cases the wet belt generates a perceptible noise. The researchers characterized basic noise properties by extensive experiments and presented mathematical models. The SAE Standard J2432 [7] entitled 'performance testing of PK section v-ribbed belts' defines the test procedure to characterize wet slip friction of belts.

These studies have not comprehensively addressed the wet belt friction mechanism. Research on the characterization and quantification of stiction (static friction) and the noise associated with wet belts is lacking yet. Wet belt noise is a critical issue for an accessory drive designer as the belt application in wet condition is not popular. This work sets out to address this issue. A set of comprehensive experiments are conducted to quantify the stiction under various influencing factors, such as wrap angle, load, acceleration, and various belt-pulley interfaces. A theoretical stiction friction model is used to study the wet belt stiction friction and quantify the effects of

parameter variations, and the model is correlated with experimental results. Moreover, noise and vibration tests were conducted and the wet noise analysis results are correlated with the stiction testing.

Regardless of the type of belt used or the size of the pulley, the friction is governed by Euler's belt equation:

$$T_1 = T_2 e^{\mu\theta} \tag{1.1}$$

where T_1 is the tension in the belt in one side of the belt,

T_2 is tension in the other side of the belt,

θ is the wrap angle formed by the belt over the pulley,

μ is the effective coefficient of friction (COF) between the belt and the pulley.

However Euler's equation is applicable only in slip conditions. In non slip condition for v-ribbed belt, Euler's equation is modified as follows:

$$\frac{T_1}{T_2} = e^{(\mu\theta/\sin(\beta/2))} \tag{1.2}$$

where β is the v angle in the v-ribbed belt.

This research deals with slip friction, hence Equation 1.2 is ignored and Equation 1.1 is used to determine COF.

Figure 1.1 shows the schematics of a typical v-ribbed belt and the belt-pulley interface. In real time applications, the wrap angle of a belt on a pulley typically ranges from 40^{o} to 180^{o}.

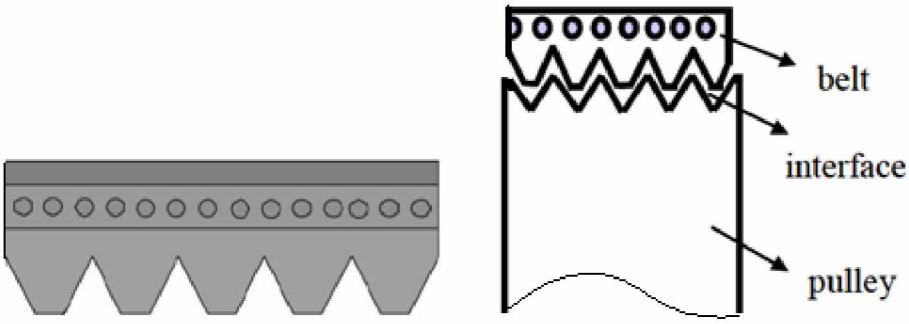

(a) Schematic of the cross section of belt (b) Schematic of cross section of belt-pulley interface.

Figure 1.1 Schematic of a v-ribbed belt and belt-pulley interface

While belt-pulley profiles can be of many types, a v-ribbed belt and its corresponding pulley are frequently encountered in automobiles. This work primarily focuses on this particular profile.

Over the last decade, the reliability and durability performance of engineering rubber materials has substantially improved due to progress in materials science and engineering. In the automotive rubber industry, a big portion of the research and development budget is spent on issues related to noise and vibrations of components and systems. Noise and vibration problems have a direct impact on customer perception of the quality of products like belts and wiper blades, and friction-related noise results in a

great amount of customer warranty cost for rubber belts. Rubber belt transmission systems are widely used in automobiles to drive automotive accessories like the power steering pump, alternator, and air conditioner compressor from a crankshaft pulley. Overload under severe conditions can lead to excessive slippage in the belt pulley interface. In poorly designed accessory systems, this in turn can lead to undesirable noise that increases warranty cost substantially. The mechanisms and data of these tribological performances, noise features and system response are of utmost interest to belt drive designers. Almost all accessory belts used in automotive engine systems have no cover. Their locations are close to the road surface and they are exposed to ambient conditions; hence the belts are susceptible to environmental effects. Thus, it is imperative to study the impact of these environmental effects in detail. The belt-pulley interface can be categorized based on the environmental conditions to which it is exposed. The experiments were conducted under the following environmental conditions:

- Dry, room temperature condition. Most belt-pulley studies have been conducted for dry interfaces as detailed in the SAE Standard J2432 [7].

- Wet interfaces are a common occurrence in most parts of the world. Presence of water in such belt interfaces generates different dynamics than absence of water [7]. The experimental setup replicates this real-time scenario and enables study of these water-affected dynamics. To further understand wet belt noise signatures, noise tests were conducted. Typically, in wet start the system had a

loud squeal clicking noise; the clicking noises occur immediately after start up. After the belt was wet by water-spraying, the wet slip noise was measured with the belt under startup operation. The sound was recorded by a microphone one meter high from the ground and one meter away from the front of the setup.

- Cold interfaces are commonly encountered in cold regions. Under such cold temperatures, the presence of water in the interface can lead to an ice film. There is a huge difference in the dynamics of dry, room temperature interfaces and liquid-state water interfaces. Similarly, frozen interfaces lead to different friction properties. These interfaces are generally encountered in cold regions where temperatures regularly fall below 0^{o}C. When a belt is used in wet, cold situations, the interface ice film is unavoidable. Although belt tests have not been conducted in cold conditions previously, there has been some research on rubber friction under cold conditions.

1.3 Outline of Research

This work has been divided into three parts: the design of a test setup, friction and noise measurements, and investigations of the data.

Design of test setup

A model has been designed and built to replicate the belt-pulley system commonly found in automobiles. It consists of a simple belt pulley system. A dead weight is attached to one end of the belt while the other end is attached to a fixed force transducer. The pulley is run by a DC motor, and resulting tensions in the belt are tabulated from the force transducer. The details are given in Chapter 2.

Friction and noise measurements

Tensions in the belt are measured for various interface conditions, various loads, and wrap angles. Based on the tabulated results, Euler's belt equation is used to determine the coefficient of friction between the belt and the pulley. Noise is measured by a microphone via a noise transducer box. The measurements are discussed in detail in Chapters 3, 4, 5, and 6.

Investigation of the data

The effect of various conditions on the COF for a given interface is observed and discussed in chapters 3, 4, 5 and 6 under the section *Discussion*.

CHAPTER 2

EXPERIMENTAL SETUP DESIGN

2.1 Introduction

All automobiles use a rubber belt to transmit power into the pulleys of various accessories in the engine. This pulley system works because of the friction between the belt and all the pulleys with which it interacts. Appropriate interaction between a belt and a pulley will result in improved efficiency. The better an accessory in the car runs, the less energy is consumed. A good belt/pulley system will result in better efficiency.

During the course of this research, the belt/pulley interface was investigated from a friction point of view. In general, there are many factors which affect system performance. Extensive research has been done on certain factors that effect the belt-pulley interaction, but certain other aspects scarcely have been investigated. Besides validating previous research in this field, experiments were conducted to study certain aspects not previously researched. The variables/factors that will be used to study friction in the interface are:

Wrap angle,

Acceleration of the pulley,

Temperature,

Tension/weight,

Presence of water/ice film.

2.2 Experimental Setup

Figure 2.1 shows a picture of the belt-pulley test rig. It consists of the two triboelements under study, a steel pulley (Triboelement 1), and a v-ribbed belt (Triboelement 2). The belt is held stationary while wrapped around the pulley at wrap angles of 81.8, 90, or 116.51. The pulley is mounted on the shaft of a DC motor. One end of the belt segment is connected to a force transducer attached to a fixed board. At the other end of the belt segment are hung dead loads of 2.5 lbs, 5 lbs, and 10 lbs, alternatively for different tests. The diameter of the pulley was 163 mm. During testing, the pulley was driven by a DC electric motor powered by a 12V battery with a speed controller. The pulley shaft rpm was measured using an optical tachometer. The running speed range was from 0-100 rpm.

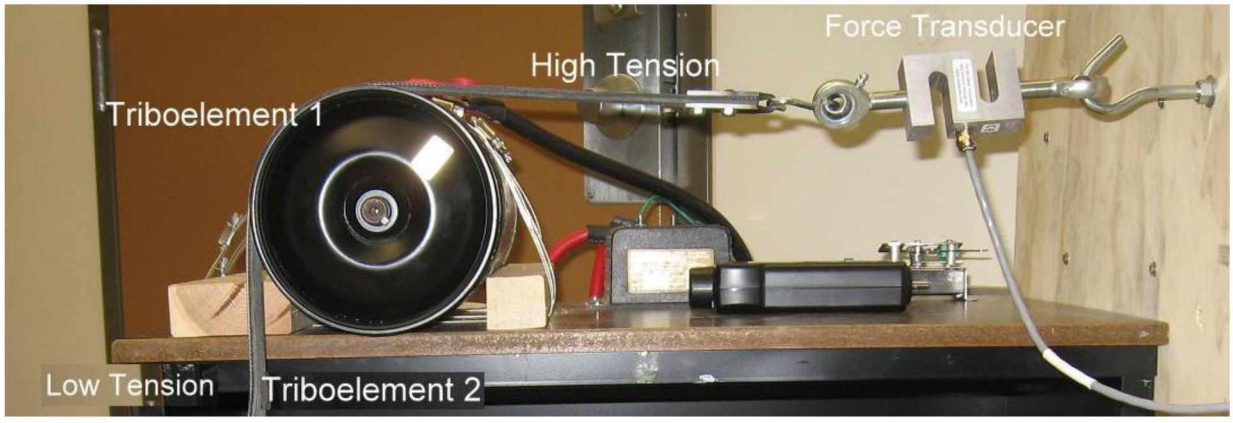

Figure 2.1 Belt-pulley test setup

The force sensor monitors the force transmitted in the belt during testing. The relationship between the forces of the tightened side and the relaxed side (dead load side) of the belt segment is established by Euler's formula (Equation 1.1). A force sensor and a data acquisition system were used to record the force history when the system was run. A load cell system (LC-105-500 Aluminum S beam load cell, and PSU-93 power supply) from Omega Company was used for force measurement, and a digital transmitter (D1521 Analog to Digital convertor) was used for outputting digital signals to the computing devise (computer). The LabVIEW VI system was used to communicate with the load cell package of Omega and to read the output signals according to the VI (Virtual Instrumentation) diagram. Measurement was conducted at room temperature of +24°C and cold temperature of -20°C. During wet testing at room temperature, both the belt contact surface and the pulley contact surface are wet prior to commencing the experiment. For cold wet testing fresh water was sprayed on both the belt and pulley contact surfaces before the motor was run, and the system was allowed to settle for some time to allow the water to freeze. A microphone was placed at a distance of 1 meter from the front of the setup at a height of 1 meter above the ground to record the noise data as well.

2.3 Material

In order to investigate the friction generated due to the rubber belt sliding on the pulley, a commercially available pulley and two types of commercially available rubber v-ribbed belts were used. Belt 1 is a Diehard Gold Company product number 464 belt while Belt 2 is a Mitsuboshi 5PK877 R34-8 belt. The steel pulley was purchased from NAPA Auto Parts, product number 611 08120. Belt 1 was used only for a few tests in Wet-Room Temperature condition for comparison with Belt 2. Almost all the experiments were conducted for the interface between Belt 2 and the steel pulley. Figure 1.1 shows the schematic of the basic construction of the v-ribbed belt and belt-pulley interface. Sample roughness was measured using an optical interferometer and a contact roughness meter. The surface mean roughness of Belt 2 is in the range of 2-6 micrometers. The average roughness of the pulley surface is about 0.5 micrometer and is considered smooth compared to the rubber belt. Figure 2.2 shows the measured roughness profile of a representative belt. The experiments were conducted both in the cold room chamber and an outdoor field under temperature of -20^{o}C. Table 2.1 presents the properties of the specimen and the interface. Both belts and pulley were purchased from automotive parts dealers, NAPA Auto Parts and Sears.

Table 2.1 Parameters of the belt-pulley interface.

Parameter	Symbol	Value
Applied load on belt	P	11.12/22.24/44.48 N
Width of belt	W	18 mm
Thickness of belt	H	6 mm
Water-belt contact angle	ϕ	60^{o}
OD of pulley	D	164 mm
RMS of belt roughness	α	2 μm
RMS of pulley roughness	σ	0.5 μm
Width of pulley	W	22 mm
Velocity	V	0-0.87 m/s

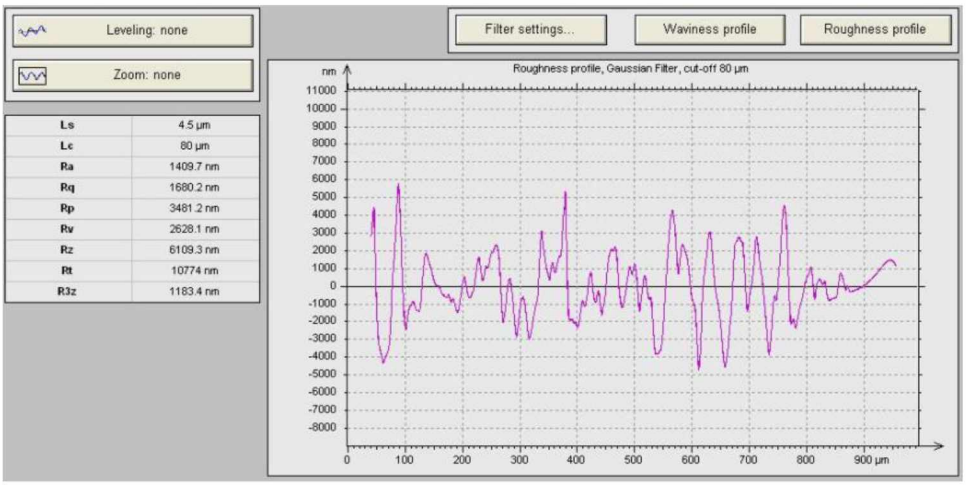

Figure 2.2 Measured roughness of a representative belt

Figure 2.3 Cold room chamber.

Figure 2.4 Photo of field testing under low temperatures.

2.4 Procedure

The following is a summarization of the test procedure:

- The desired interface is first developed. Four types of interfaces are studied in this research: dry-room temperature (Chapter 3), wet-room temperature (Chapter 4), dry-cold temperature (Chapter 5), and wet-cold temperature (Chapter 5).
- The belt is loaded with the desired weight at one end and is connected to the force transducer at the other. It is wrapped over the pulley at the desired wrap angle.

- The circuit breaker is activated, and all connections are secured.
- The LabView program is run (to record readings from the force transducer).
- The Audacity program is run to record noise from the microphone.
- The speed control is set to the desired rpm setting.
- The computing device records all necessary values from the input devices.
- The speed control is set to zero and the system is brought to a stop.
- The readings are saved in appropriate formats.

Readings recorded during the experiment are of Tension and Sound.

Tension

As mentioned above, one portion of the belt has constant tension (due to the load hung from it), while the tension in the other portion changes as the experiment proceeds. When the speed control is turned on, the motor shaft begins to turn and consequently the pulley turns. Due to the friction generated between the belt and the pulley, the frictional force tries to move the belt along with the pulley. However, with the belt being restrained at one end (connected to the wall via the force transducer), the resulting frictional force is transmitted to the belt portion between the pulley and the wall. This causes an increased tension in the belt. The force transducer then records these values of tension versus a time scale depending on the need for accuracy. The time scale chosen for the experiment records the tension values (in lbs) for every 101 ms. Euler's belt

equation is then used to calculate the COF for the given interface for the given conditions.

Sound

Sound emanating from the interface due to friction is also recorded via the use of a microphone connected to an amplifier. As mentioned earlier, the microphone is placed one meter from the test setup and one meter above the ground. A different computing device is used to record these sounds than that used for LABView. Audacity is the software used for recording these sounds. The effects of various conditions/variables (individually or in combination) are observed and studied.

CHAPTER 3

DRY FRICTION AT ROOM TEMPERATURE

3.1 Introduction

The aim of this research is to study a rubber belt-pulley interface under various environmental and operational conditions. Most previous research on rubber belt friction studies the same in conditions that can be considered relatively dry and operating at temperatures above 0^{o}C [1-7]. As a fully viscoelastic frictional material, rubber friction has been widely investigated [8-11].

A series of experiments were conducted inside a closed laboratory replicating the dry-environment scenario. The temperature inside the laboratory was found to be 24^{o}C while relative humidity levels were measured to be around 30% (low enough to be considered a dry atmosphere). The COF data obtained from the experimental test setup is grouped into regimes based on wrap angles and dead loads attached to one end of the belt. The loads are 2.5 lbs, 5 lbs, and 10 lbs; the wrap angles are 81.8^{o}, 90^{o} and 116.5^{o}.

3.2 Effect of Varying Wrap Angle

As mentioned earlier, the setup was tested for three varying wrap angles (81.8°, 90o and 116.5°). Upon closer inspection of the results, Figures 3.1-3.3, it can be seen that at 90° wrap angle, the COF value is slightly higher (1.35) than those recorded for the same load at 81.8° and 116.51° wrap angles (1.25). For each wrap angle, 3 experimental trials were conducted for 2.5 lbs dead load and the results were extremely close to each other, with the maximum variation (seen in Figs. 3.1 & 3.2) of less than 8 % within each set. This low variation % illustrates that the COF is stable and results from the test setup can be considered accurate. The belts used in the testing process have been run hundreds of times.

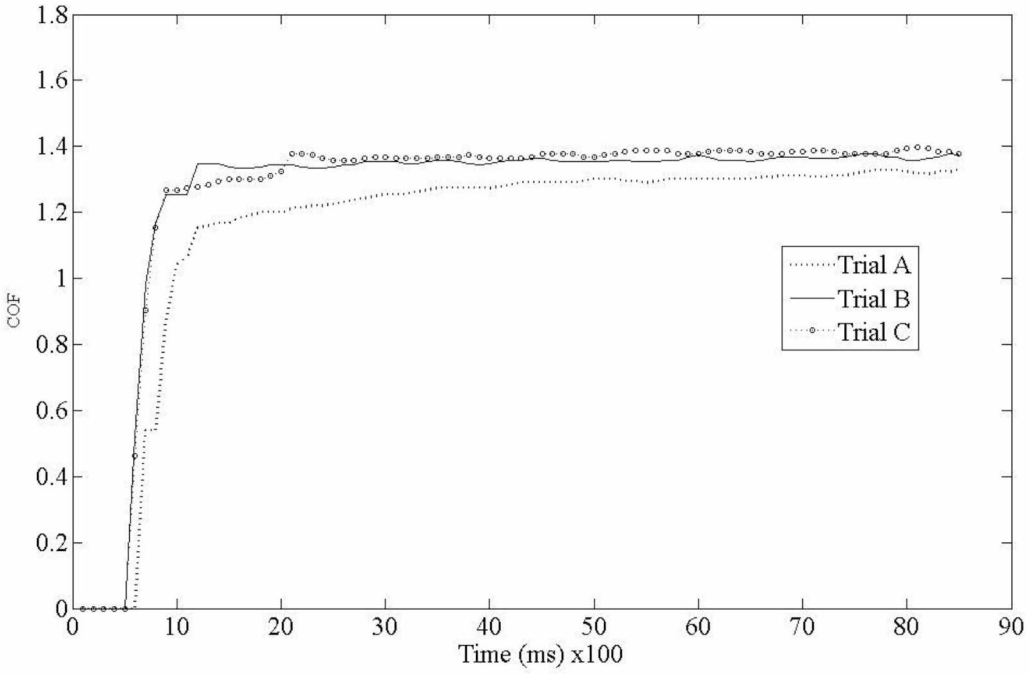

Figure 3.1 COF vs. Time for 2.5 lbs load & 90° wrap angle (dry, room temperature)

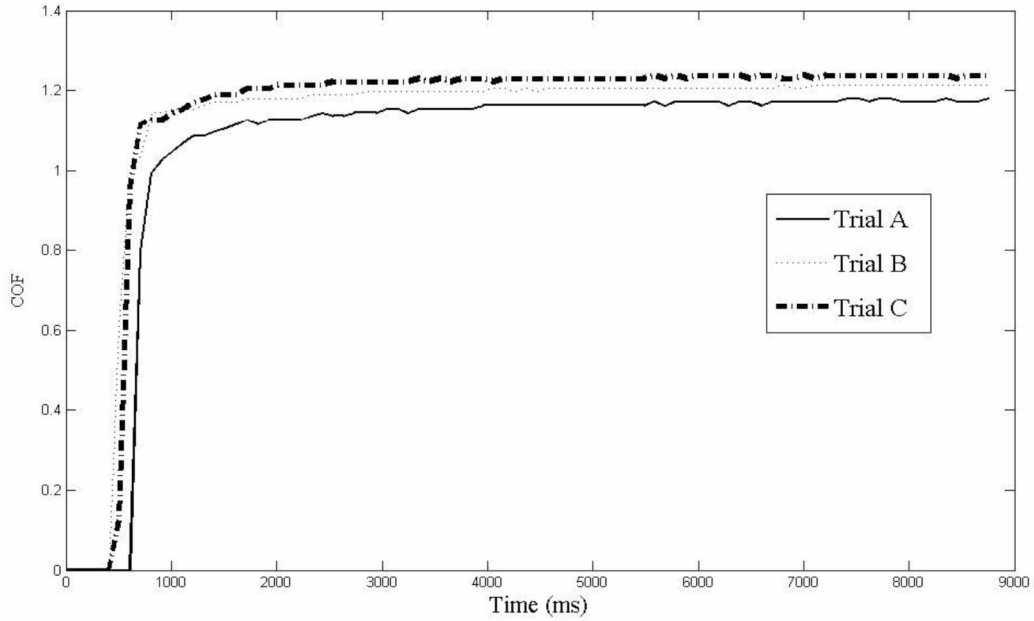

Figure 3.2 COF vs. Time for 2.5 lbs load & 81.8^{o} wrap angle (dry, room temperature).

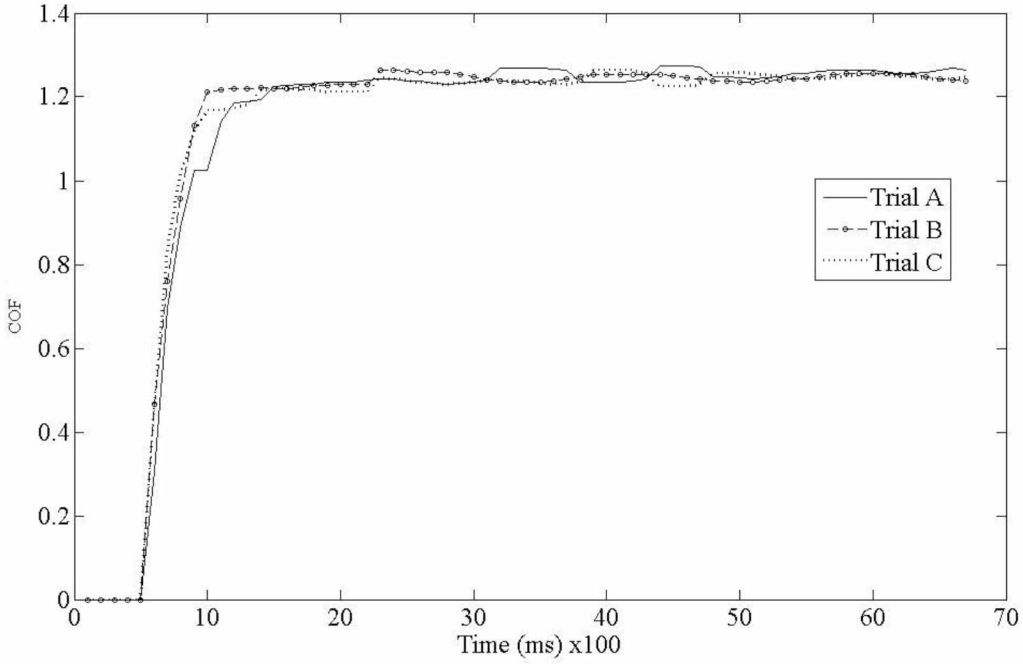

Figure 3.3 COF vs. Time for 2.5 lbs load & 116.51° wrap angle (dry, room temperature).

3.3 Effect of Varying Dead Load

Another aspect under study is the effect of varying the dead load attached to one end of the belt. In this case, while keeping the wrap angle the same (90^{o}), three different sets of experiments were conducted each with a different dead load: 2.5 lbs, 5 lbs, and 10 lbs dead load. The rest of the conditions (dry, room temperature) were also left unchanged. The results are shown in Figures 3.1, 3.4, and 3.5.

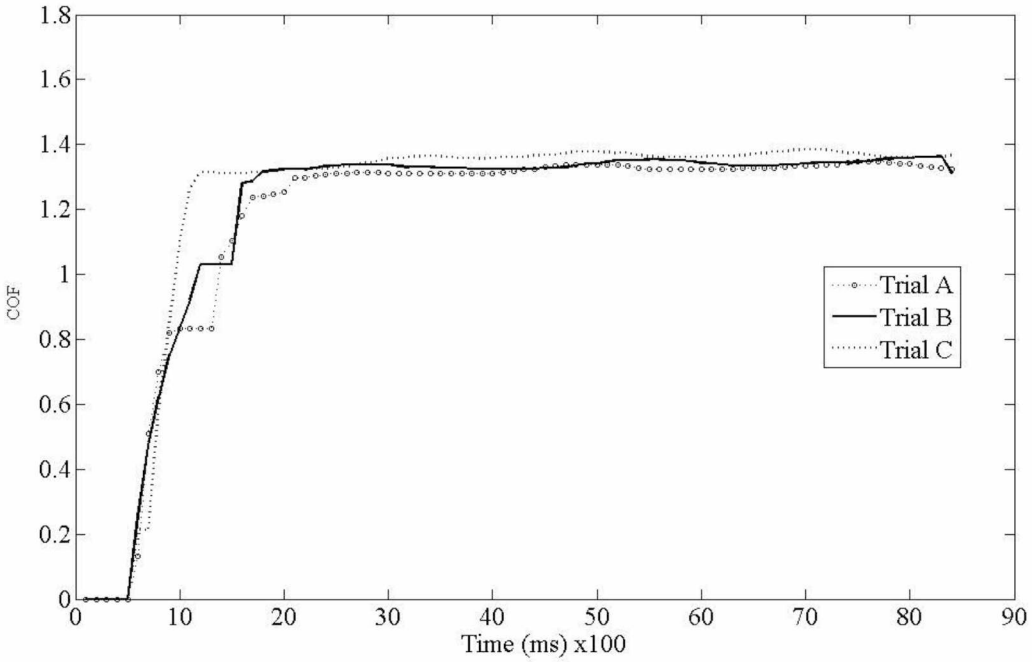

Figure 3.4 COF vs. Time for 5 lbs load & 90^{o} wrap angle (dry, room temperature).

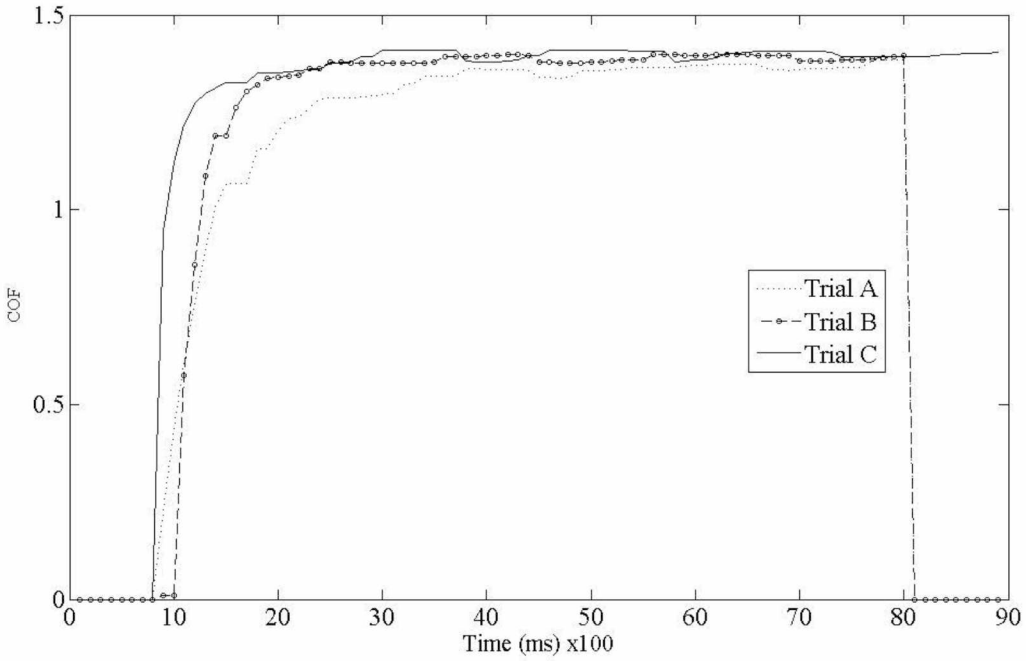

Figure 3.5 COF vs. Time for 10 lbs load & 90^{o} wrap angle (dry, room temperature).

Noteworthy that once again the variation in COF seen in the results within each set is very low.

3.4 Effect of Varying Acceleration

A manual speed control was used to run the motor and generate the readings under varying conditions. One of the unique aspects of this test setup is the varying acceleration generated by the speed control. Due to the speed control being analog, there was no definite way to measure the acceleration of the motor shaft (and thus the pulley). However, a rough method was used to visualize two varying acceleration conditions. A point was marked on the speed control, upon reaching which, the pulley was determined to have a rotation speed of 100 rpm. The time taken to reach this point was used to determine the two varying acceleration conditions: (1) the time taken was less than 4 seconds and (2) the increase in pulley rpm was more gradual (the time interval could not be determined with certainty since a frozen interface takes more time than a non frozen interface in this acceleration condition). It suffices to know that the second condition takes enough time to generate varying results from the first acceleration condition. For future reference and to avoid confusion, the first case is referred to as quick acceleration, the latter as slow acceleration. The varying acceleration has small effect for dry interfaces as seen in Figure 3.6 of the three trials: Trial A and B was quick acceleration where as trial C was slow acceleration. Similarly, each set of data from the dry, room temperature tests has two quick acceleration tests and one slow acceleration test. For dry-room temperature scenario, the quick and slow acceleration trials are almost indistinguishable. There is no significant difference in the three trials within each

set. This lack of difference can also be seen in dry-cold conditions for varying accelerations as will be seen in Chapter 5.

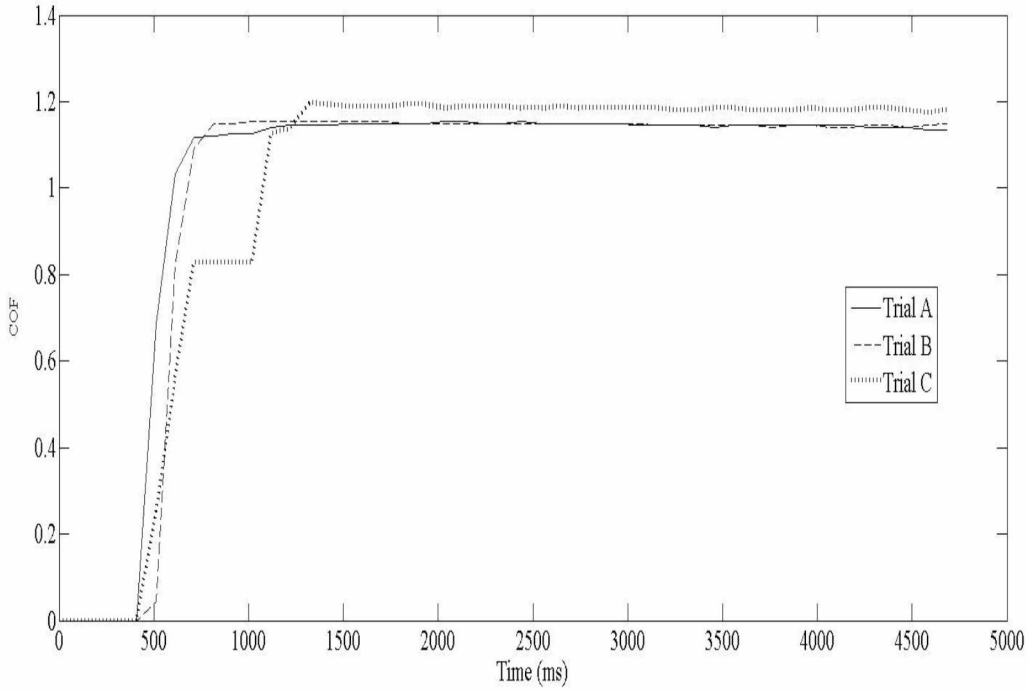

Figure 3.6 COF vs. Time for 5 lbs load & 81.8^{o} wrap angle (dry, room temperature).

By comparing Figures 3.4, 3.6 and 3.7, the effect of varying wrap angle for 5 lbs load can be noticed. It follows a similar pattern as for 2.5 lbs; i.e., a slightly higher COF value is observed for 90^{o} wrap angle (Fig. 3.4) as compared to 81.8^{o} and 116.51^{o} (Figs. 3.6, 3.7). A similar pattern is observed for 10 lbs load (Figs. 3.5, 3.8 & 3.9).

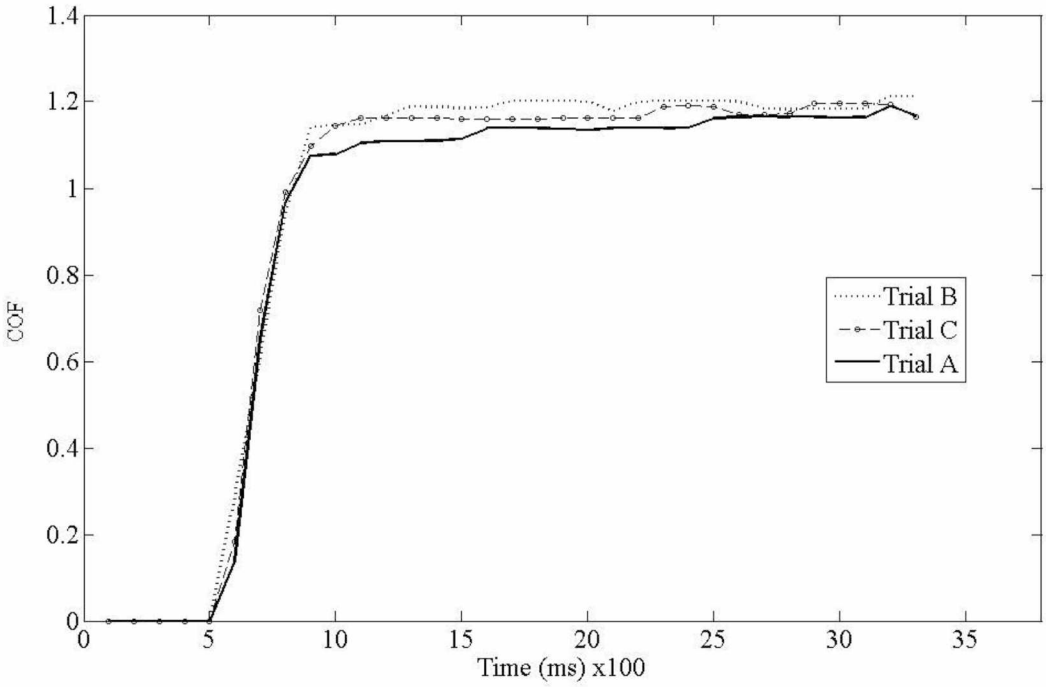

Figure 3.7 COF vs. Time for 5 lbs load & 116.51° wrap angle (dry, room temperature).

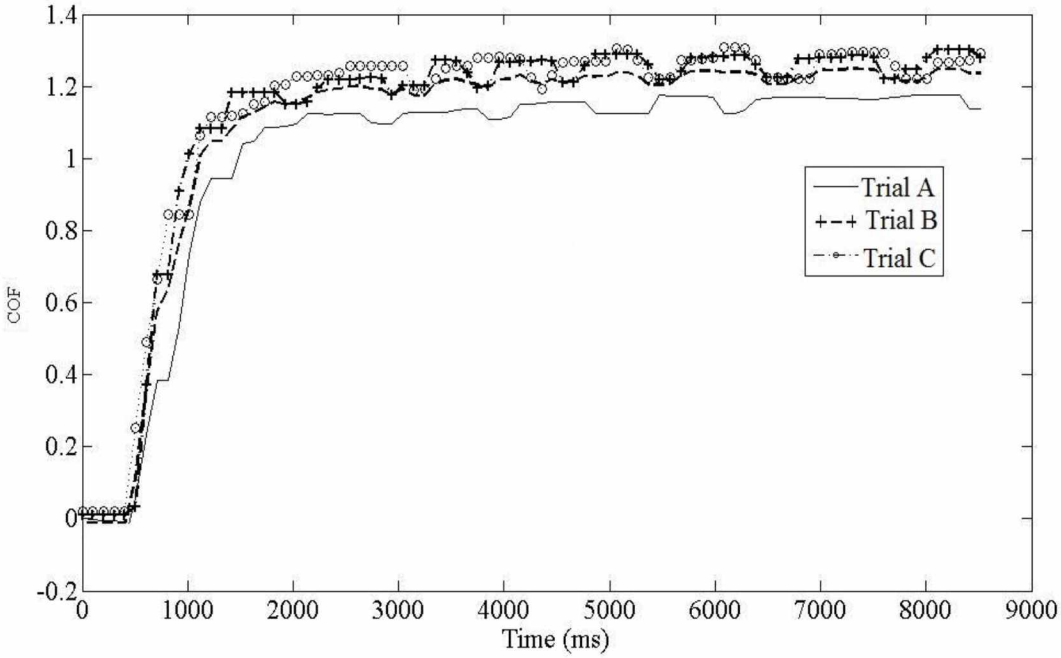

Figure 3.8 COF vs. Time for 10 lbs load & 81.8^{o} wrap angle (dry, room temperature).

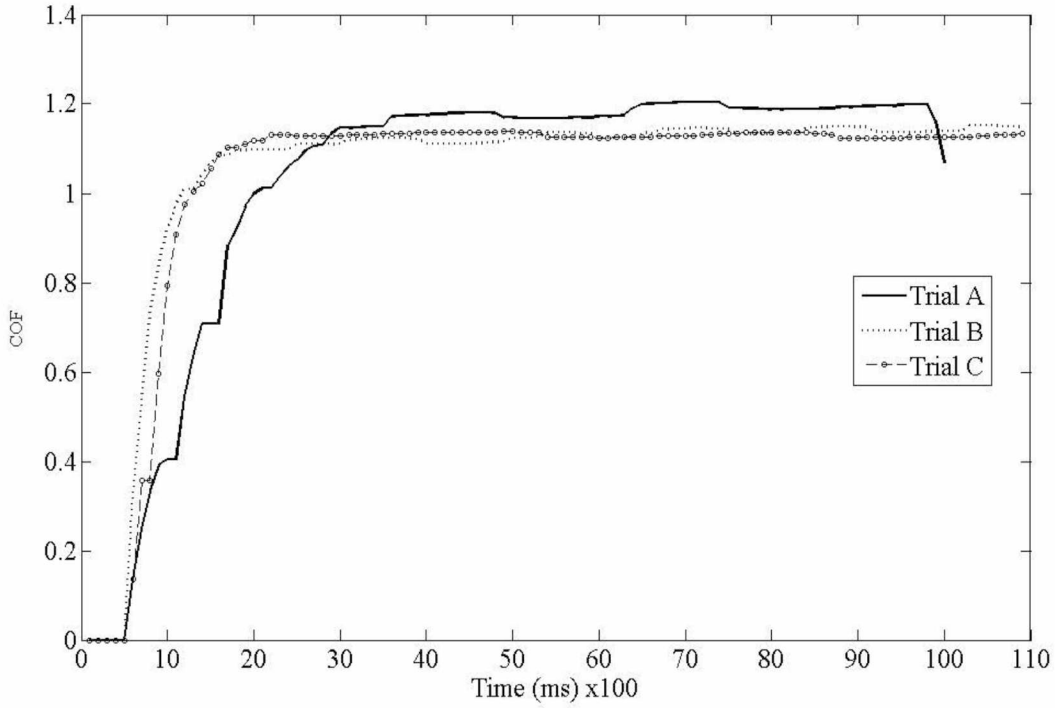

Figure 3.9 COF vs. Time for 10 lbs load & 116.51^{o} wrap angle (dry, room temperature).

3.5 Discussion

Based on existing research [8, 9, 12-14], for rubber in sliding contact with metal, the combined effect of adhesion and internal damping contributes to friction. In sliding, adhesion acts at the contact area, whereas strain develops within the rubber and leads to the buildup of elastic energy. When the elastic stress exceeds the adhesive force, breakage of the contact bond takes place and sliding occurs. The adhesion then moves to a new area and so on. For rubber sliding on a clean rigid surface, it was reported that there exist waves of detachment, which traverse the contact area from front to rear or from compression side to tension side at a very high speed. The driver for the waves of the detachment is the tangential stress gradient. There is continuous and alternative de-attachment and re-attachment passing through the contact area. Generally, the static friction is fully due to adhesion, whereas the internal damping effect starts to contribute to friction after belts start to slide.

Unlike the contact of two hard surfaces, in which the area of real contact consists of randomly distributed junctions where the surface asperities of the two surfaces interact to cause deformation, the contact between rubber and a hard surface is quite different. Persson pointed out that when rubber slides at low speed on a polished glass surface, rubber in the contact area will deform to follow the short-wavelength surface roughness profile of the glass substrate because of adhesion to the hard substrate [8, 9, 12-14]. The real contact area with rubber is much larger than that of the two hard surfaces. In the belt-pulley interface, since the contact pressure is relatively small, belt

rubber is relatively rigid, and the roughness of the pulley is substantially higher than that of glass, we can assume that the rubber in the contact area deforms in a way to properly follow the short-wavelength roughness profile of the pulley with some cavities as illustrated in Figure 3.10. Basically, the rubber belt penetrates into the valley of the pulley surface, which may leave some cavities between the belt and pulley surface.

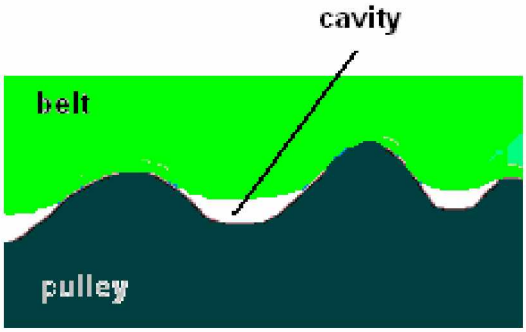

Figure 3.10 Schematic of dry rubber belt on a pulley surface.

When rubber is in contact with a hard surface, rubber can deform elastically to establish an actual area of contact that is equal to the nominal area of contact for large contact pressures and a relatively smooth surface. The friction of rubber increases with the nominal area of contact. When rubber slides on a rough, hard surface, the surface asperities of the hard surface exert oscillating forces on the rubber surface leading to energy ‘‘dissipation’’ via the internal friction of the rubber. During sliding the asperities of the rough surface exert alternative compressive force and release force transients on the rubber surface, leading to cyclic deformations of the rubber and energy dissipation through the internal damping of the rubber. Viscoelastic effects have been estimated by quantifying the energy dissipation in a viscoelastic material; the energy dissipation is

then used to estimate the contribution from the internal friction to the sliding friction. The large fraction of rubber friction has been attributed to energy ''dissipation'' occurring in the bulk of the rubber due to the fluctuating surface stresses acting on the rubber from the surface asperities of the hard surface. A general formula for rubber friction can be written to show that the coefficient of friction is proportional to the imaginary part of the complex elastic modulus of rubber; it is inversely proportional to the modulus of the complex elastic modulus, evaluated at a specific frequency defined by the ratio of sliding velocity to the size of the asperity contact area [9, 10, 14, 15]. A model of the adhesive friction of rubber is given as follows:

$$\mu = \alpha(A/P)\tau \tan\delta \tag{3.1}$$

in which μ is the coefficient of friction, α is a constant, A is the contact area, P is the load, τ is the shear stress, and δ is the tangent modulus.

The value (P/A) is also known as contact pressure. Equation 3.1 also explains to a certain extent the variations in COF due to varying parameters (wrap angle, dead load). In the equation, it is assumed that δ is constant with respect to load applied or the wrap angle. Contact area changes as the wrap angle is changed: an 81.8^{o} wrap angle has less contact area than a 90^{o} wrap angle which in turn has less contact area than a 116.51^{o} wrap angle. Thus, a higher wrap angle results in larger COF for the same load applied, as seen in the results in Figures 3.1 and 3.2. The former is the result for a 90^{o} wrap angle while the latter is for an 81.8^{o} wrap angle. However, Equation 3.1 cannot account for the variation between the results in Figures 3.2 and 3.3 (wrap angles of 90^{o} and 81.8^{o},

respectively). This can be due to the fact that the Equation 3.1 is only a theoretical model given by Persson [9, 10, 14, 15], and cannot be assumed as a definite guideline for the results from the current research. Maintaining a constant wrap angle but increasing the load increases the contact pressure value as well as the shear stress. Since the increase in contact pressure is countered by the increase in shear stress, the friction values should remain unaffected. Comparing Figures 3.4 and 3.5, it can be observed that the former (5 lbs & 90^{o} wrap angle) shows a slightly smaller COF value as compared to the latter (10 lbs & 90^{o} wrap angle). This discrepancy from the equation can be explained by the fact that increasing the contact pressure could lead to more surface contact area between the belt and the pulley, thereby increasing the friction. However, on comparing the result in Figures 3.7 and 3.9, the opposite phenomenon is observed, kinetic COF decreases with increase in load. Overall, Equation 3.1 can be considered a probable guideline for such testing procedures as in the current research; however, as mentioned before, since it is just a theoretical model, it cannot be used as a definitive guideline. Furthermore, due to the variation of wrap angle and/or dead load the deviations between each set are relatively small compared to the COF values themselves. The COF values remain fairly constant despite varying the parameters.

Because of its viscoelastic nature, rubber at low sliding velocities tends to flow or creep over a surface just as a viscous liquid flows smoothly around objects. Friction in this creep region tends to increase with speed. After velocity increases into the relatively high speed level, the friction values could be leveling off as the rubber is no longer able to maintain proper contact with the pulley.

3.6 Conclusion

Based on the pulley parameters and the rpm at which the pulley is run, the maximum velocity of the belt has been calculated at close to 0.9m/s (Table 2.1) which is considered a high speed level. In terms of the present test results, the conventional theoretical model and observation mentioned above can be considered valid for dry rubber belt-pulley interface. The deviation % observed in the results obtained for varying criteria is small enough to be negligible.

CHAPTER 4

WET FRICTION AT ROOM TEMPERATURE

4.1 Introduction

The robustness and noise warranty costs of rubber belts used for power transmission are directly affected by frictional properties under varied environmental conditions. In practical applications, start-up running or overload torque often causes tangential slippage between belt and pulley. Wet conditions can increase the slippage substantially and cause noise. This chapter presents an experimental characterization and analysis of the friction behavior of automotive v-ribbed rubber belts under wet conditions. The presented results are based on the start-up running of the belt-pulley test rig and differ from some published results based on SAE Standard J2432 [7]. The test rig based on SAE Standard J2432 is actually operated as water-lubricated coast-down, which is not applicable to characterizing the friction properties of belt in wet start-up running.

The presence of water or high moisture on belts is unavoidable under rainy weather conditions, which usually induces greater slippage as the water film in the interface changes the friction mechanisms in the interface from Coulomb friction to boundary lubrication and even mixed lubrication [16]. The rubber-friction of mixed lubrication has been found to exhibit a negative slope of the curve of coefficient of

friction (COF) versus velocity, i.e. friction has been found to increase with speed at higher speed levels. It has been reported that the wet friction of belts with a negative slope of COF-velocity curve can lead to self-excited vibrations and squeal noise. Conventionally, the wet friction of belts has been characterized by using the standard test rig and procedure defined in SAE J2432 [7]. Some published literature on the noise and tribological properties of wet belts were based on experiments using the SAE test rig. Published experimental results show that wet belt slip could induce noise for some applications. Meckstroth and Ahoor studied the tribological and dynamic properties of belts under dry and wet conditions [1, 2]. Connell and Rorrer investigated friction-induced vibration and noise in v-ribbed belt applications [3]. Dalgarno, Moore, and Day studied noise due to tangential slip of v-ribbed belts [4]. Sheng et al. investigated friction-induced vibration and noise of v-ribbed belts under wet conditions [5, 6]. They characterized basic noise properties by extensive experiments and presented mathematical models. The standard SAE J2432 defines the test procedure to characterize wet slip friction of belts [7] and has been widely used. However, the procedure of SAE J2432 uses coast-down instead of start-up running for testing. Moreover, the related standards and studies on wet friction and noise used exaggerated wet conditions by continuously supplying water onto the interface when the belt was running under high speeds. This abundant water supply condition helps to define the worst threshold for slippage occurrence when the belt is running. However, it does not represent the real condition of wet belt start-up running in which the belt is accelerated from stationary to full speed. In wet start-up operation, the interface is under the fully

wet condition only at the beginning: water is not supplied continuously. In previous research works, the wet slip noise measured using the SAE test rig has been attributed to the negative slope of the friction-velocity curve. The larger static friction in start-up was only hypothesized as a possibility, which was not observed from the SAE test rig. Research on characterizing and quantifying wet belt static friction and the associated noise in start-up running is lacking. It was reported that many belts develop a noise problem during wet start-up running [8]. This kind of wet friction noise sustains for a short period only and will die away after the system dries up. Since this type of phenomena directly affects customer perception of product quality and causes warranty cost, it has received wide attention. However, this kind of start-up condition cannot be accurately simulated by the SAE test rig due to its operational limitations. The SAE test rig always maintains the test belt running at specified high speeds by a driving pulley, and it characterizes belt friction by braking a driven pulley and measuring the brake torque, which actually quantifies the friction for the coast-down process.

Persson has conducted many fundamental researches on rubber friction [9, 10]. When rubber, a fully viscoelastic material is in sliding contact with a metal surface, the combined effect of adhesion and deformation contributes to friction. Persson illustrated that when rubber slides on a wet hard substrate, the sliding friction is reduced as the water is trapped in the surface cavities of the substrate leading to reduced viscoelastic deformations of the rubber [9, 10]. Roberts investigated water entrapment with slowly moving elastic surfaces [13]. Persson provided some understanding of liquid entrapment phenomenon in the context of tire application [14, 17]. Koenen and Sanon [16]

investigated the friction of a rubber blade on wet glass. They discussed the influence of velocity on the friction coefficient of a rubber wiper blade under wet condition and the associated noise. The friction of the wet rubber blade-glass interface exhibits both boundary lubrication and mixed lubrications. The friction of boundary lubrication at low speed has been found to be less than the dry friction.

This chapter provides an experimental characterization and analysis of the friction of rubber belts under wet conditions. In this study, the test rig was used to characterize the friction of a wet belt-pulley interface under start-up running. Both belt and pulley contact surfaces were wet separately then brought in contact.

4.2 Wet Friction

The wet trials were initially intended for two different belt types – Belts 1 and 2 (Section 2.3); however, Belt 1 could not be used for all testing conditions as was planned. The forces generated in the belt exceeded the force transducer's maximum limit for certain dead load and/or wrap angles. No such problems were encountered for Belt 2, though one testing criterion that was successfully conducted on both belt types was used to show the difference between the two types (Fig. 4.2). The dotted line in Figure 4.1 shows the experimentally measured belt force/tension history of Belt 1 under wet start-up running condition. The original force acting on the belt is 23N (5 lbs) due to dead load at 90^{o} wrap angle. When the pulley is driven to rotate, it applies a frictional force on the belt, which causes an increase of the tension in the belt. This is shown as

wet static friction in Figure 4.1 where there is an abrupt increase of the force. The wet friction exhibits a peak at the beginning, and then it drops quickly to a much lower level, which reflects the wet kinetic friction. The salient static friction peak was only observed for wet belts hence depicting the typical capillary effect. For comparison, the solid line in Figure 4.1 shows the measured dry friction force in contrast to the wet friction force. It can be seen that the wet static friction is obviously higher than the dry static friction. It can also be seen that there is no peak for the dry static friction, as the dry static friction is less than the dry kinetic friction. Figure 4.2 shows the measured wet friction force history for the two different belts, for 5 lbs load at 90^{o} wrap angle. Belt 1 is the same belt reported in Figure 4.1, a lightly conditioned belt by a few test runs. Its static friction is higher than the kinetic friction by 40%. Belt 2 is different belt from a different company also lightly conditioned with a few dozen test runs (Section 2.3). Belt 2 was tested for two different acceleration conditions – slow acceleration and quick acceleration (Section 3.4). Its quick acceleration static friction is larger than the kinetic friction by 40%. The measured static wet frictions depend on many test conditions, such as wrap angle, dead load, and acceleration. The wet static friction of Belt 2 under slow acceleration is also plotted and is higher than kinetic friction by nearly 60%. It can be seen that a high acceleration leads to a lower static friction.

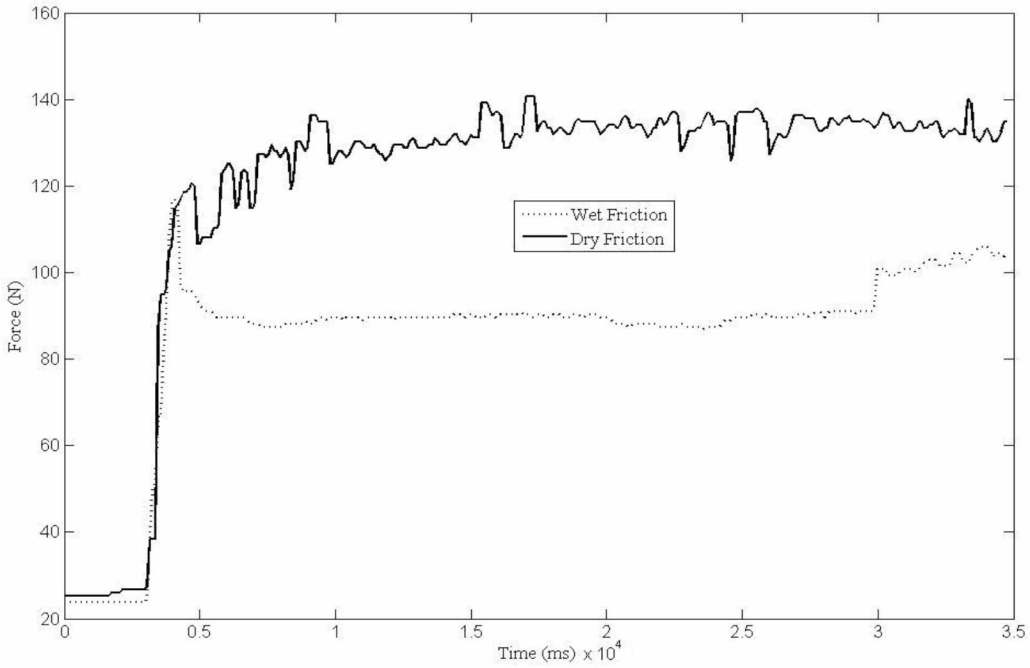

Figure 4.1 Measured static and kinetic tangential force history under dry and wet conditions.

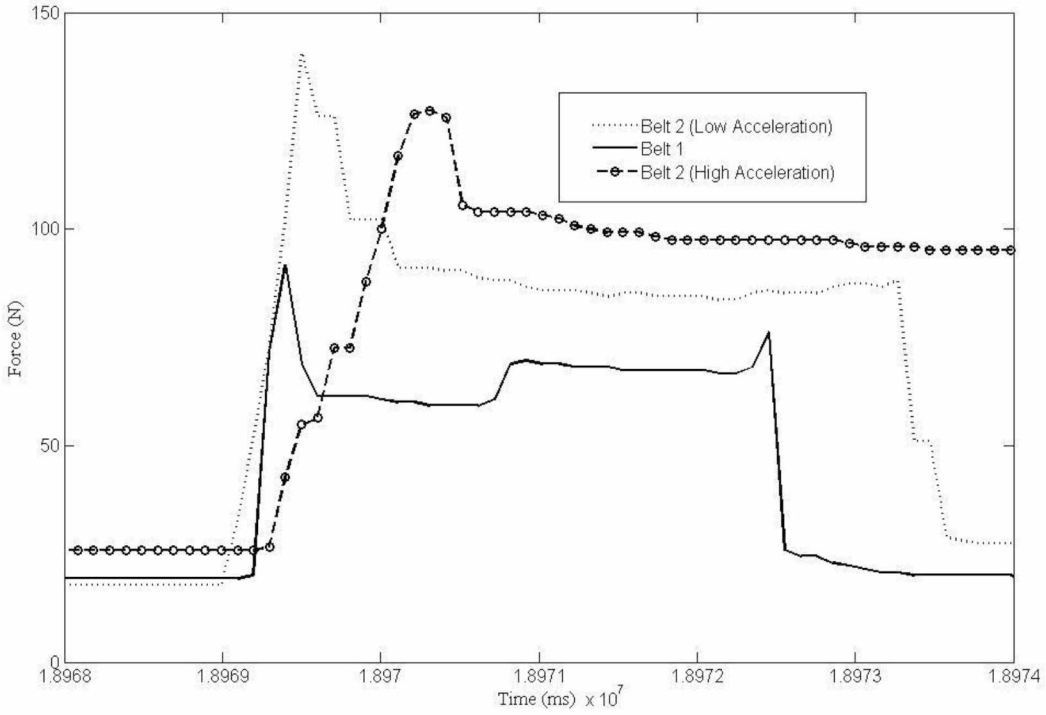

Figure 4.2 Measured wet friction force history for two belt types (Belt 1: static friction is larger than kinetic friction by 40%; Belt 2: quick acceleration static friction is larger than kinetic friction by 40%; slow acceleration static friction is larger than kinetic friction by 60%).

Figures 4.3 – 4.5 show the results from tests conducted on Belt 2 at room temperature for various testing parameters under wet startup condition. Each result set is further differentiated with in itself based on quick or slow acceleration trails. The trend between the two acceleration types is similar to that observed in Belt 2. In Figure 4.3, Trials A and B are slow acceleration tests while Trials C and D are quick acceleration tests. The difference between static wet COF values and kinetic COF values is larger in the case of slow acceleration than that of quick acceleration. Also, the kinetic COF values show a substantial difference between slow and quick acceleration trials with the former

consistently showing higher values. The same trends are observed in Figures 4.4 and 4.5.

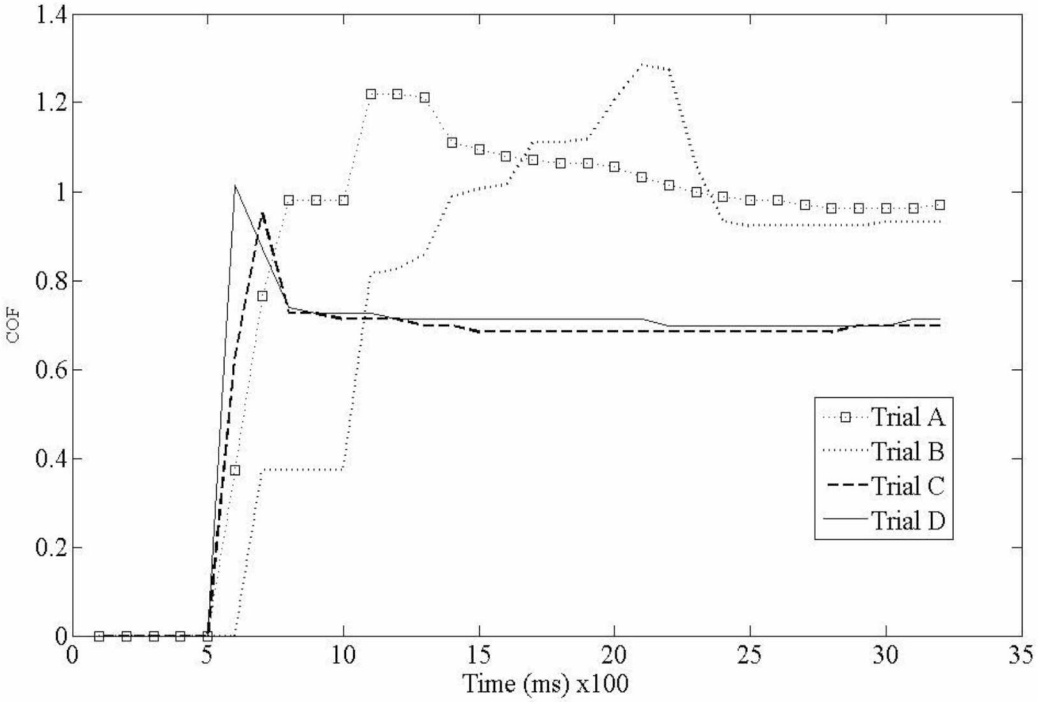

Figure 4.3 COF vs. Time for 2.5 lbs load & 90^{o} wrap angle (wet, room temperature).

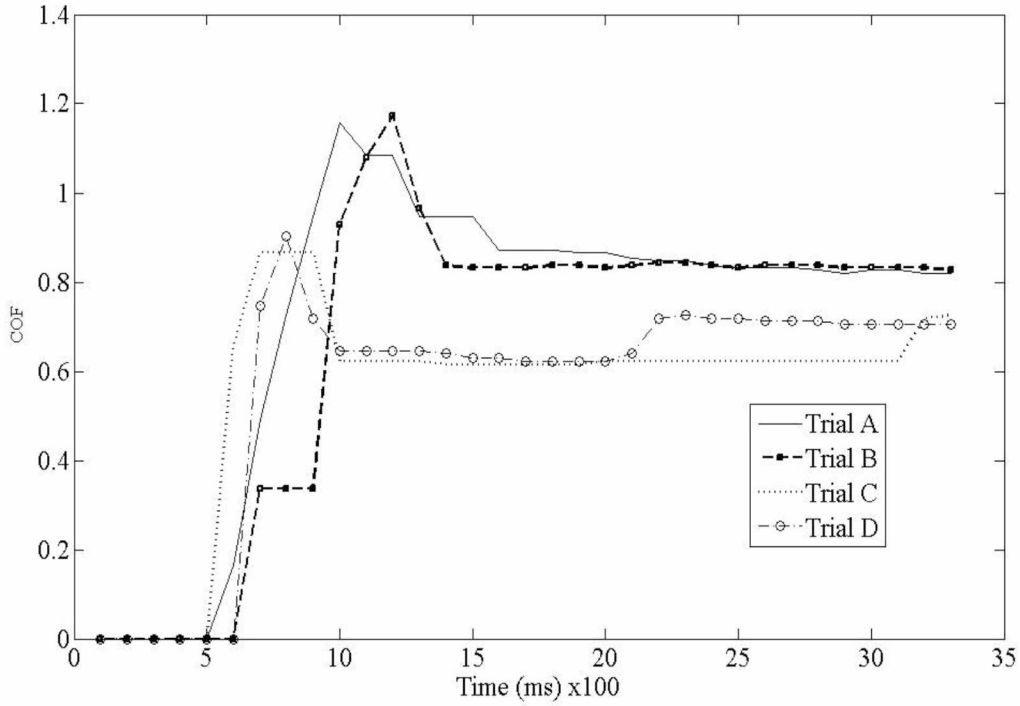

Figure 4.4 COF vs. Time for 5 lbs load & 90^{o} wrap angle (wet, room temperature).

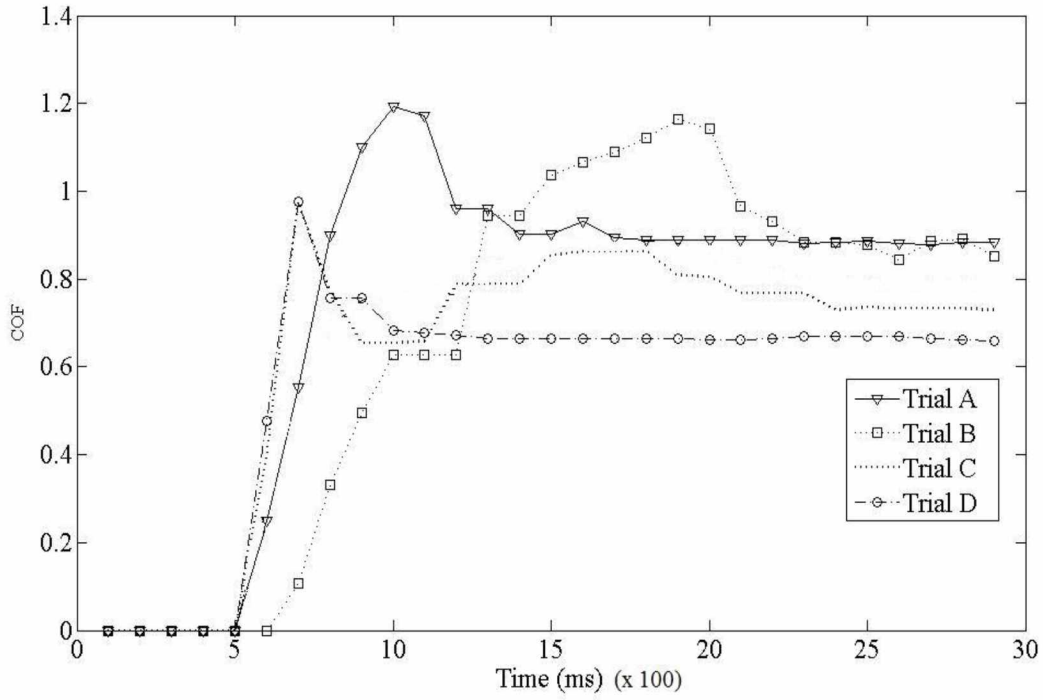

Figure 4.5 COF vs. Time for 10 lbs load & 90^{o} wrap angle (wet, room temperature).

This work is not an extensive investigation to get the best results from a certain sample for optimal design. The emphasis is instead on describing and interpreting general friction behavior, pointing out trends and related vibro-acoustic properties for future investigations, modeling, and development.

4.3 Wet-to-Dry Friction

The purpose of this experiment is to investigate the friction properties of an initially wet belt that is run till the interface turns dry. For this experiment, the belt-pulley interface was initially wet, and a series of experimental runs were conducted with brief intervals of time between each run. The experiment was conducted at room temperature, and the parameters were set at 2.5 lbs dead load and 90^{o} wrap angle. The interface was not altered in any way once the experiment started. A total of 16 runs were executed over a period of 24 hours with certain intervals extending several hours and certain intervals lasting as little as 2 minutes. This variation in time intervals was done in order to look into a real-time scenario where the belt-pulley interface develops from wet to dry. Initial runs showed results similar to wet friction results, a stiction peak followed by a kinetic friction. It is worth noting that as the runs proceeded, for the initial 5 runs, both the stiction values and kinetic COF values showed no significant change, indicating a wet interface throughout the initial phase of the experiment. Another interesting phenomenon is that a distinctive stiction effect was observed at the end of each trial although it had lower peak than that observed at the beginning of the trial.

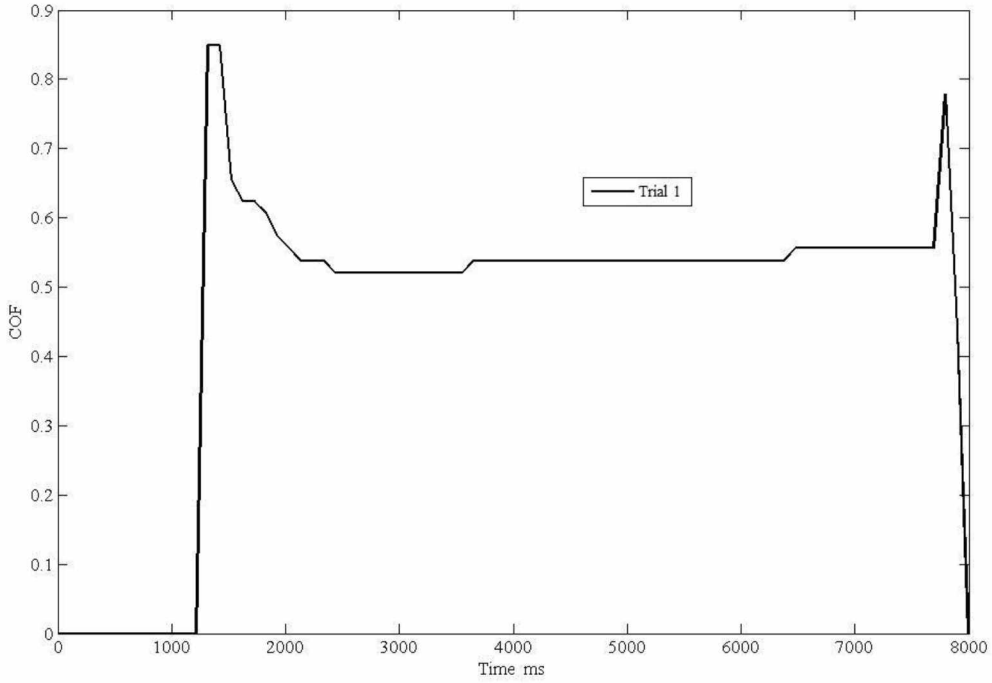

Figure 4.6 COF vs. Time for 2.lbs & 90^{o} wrap angle (wet-to-dry, room temperature).

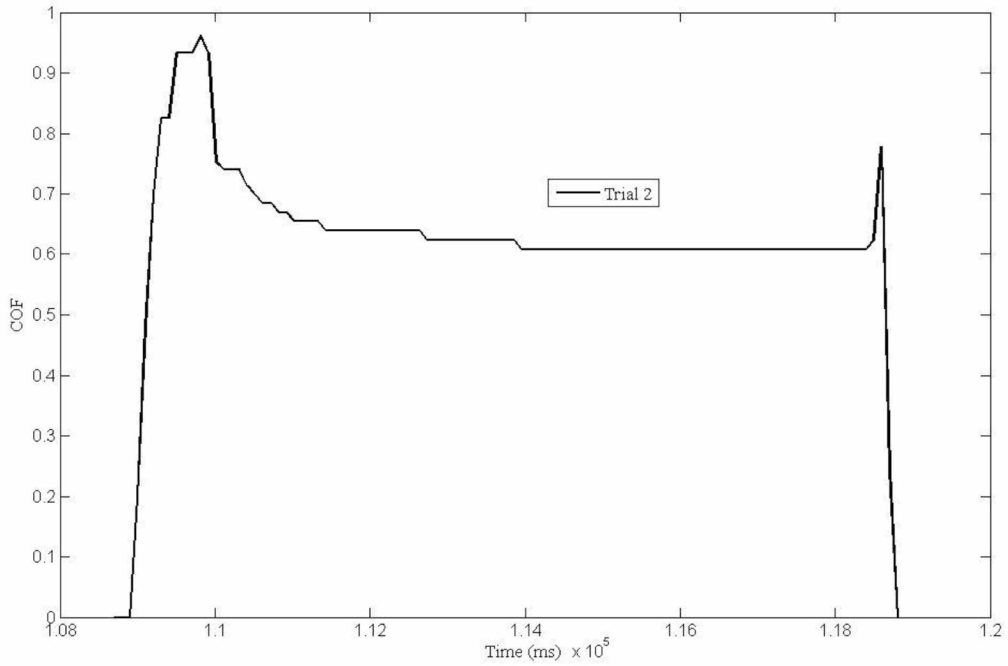

Figure 4.7 COF vs. Time for 2.5 lbs & 90^{o} wrap angle (wet-to-dry, room temperature).

The next batch of tests was conducted with an interval of 3 hours between the 5th and 6th trial. A significant change was seen. Both stiction and kinetic COF values showed no significant change from previous results (compare Figs. 4.8 & 4.9 with Figs. 4.6 & 4.7). The stiction peaks were still seen due to the interface not being completely dry (there appears to be some water left in the interface, showing certain wet friction characteristics). However, a significant difference between the initial phase and the second phase of the experiment was the lack of a stiction peak at the end of each trial in Trials 6-10 compared to Trails 1-5.

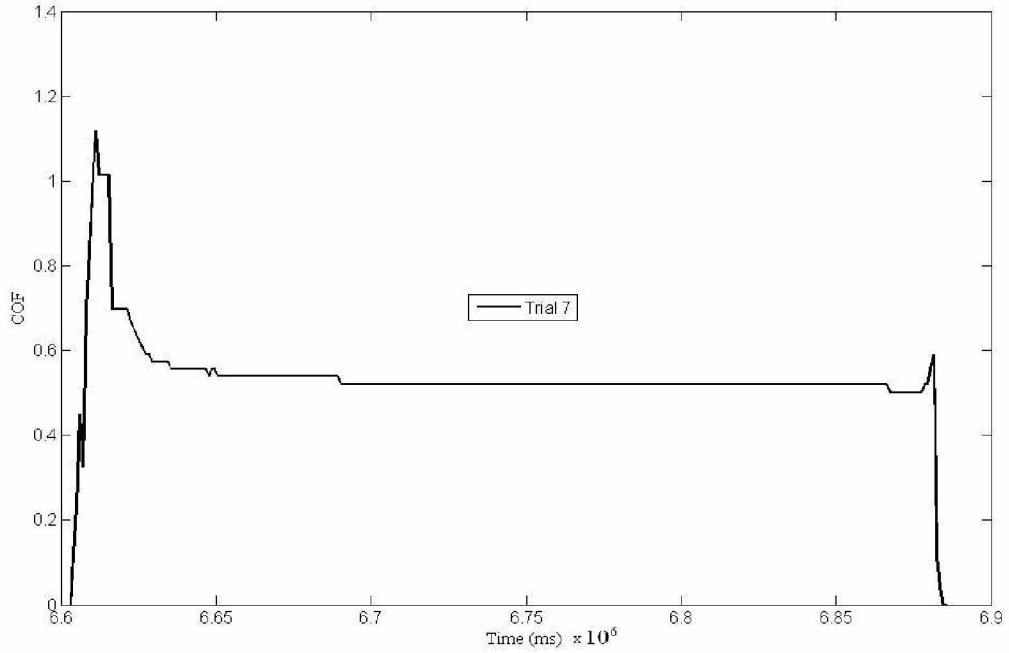

Figure 4.8 COF vs. Time for 2.5 lbs & 90° wrap angle (wet-to-dry, room temperature).

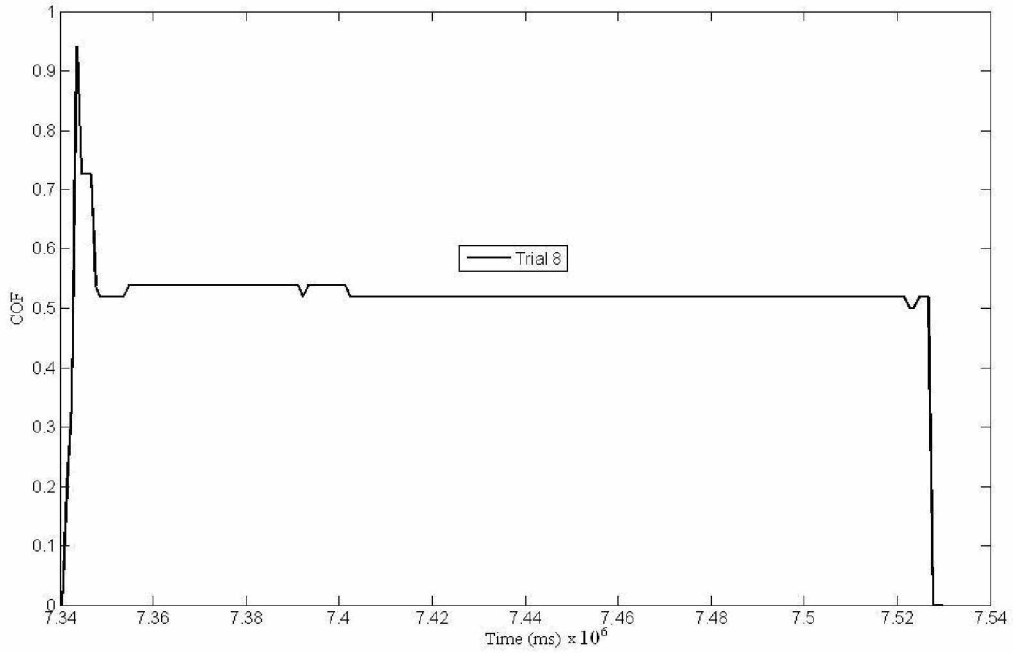

Figure 4.9 COF vs. Time for 2.5 lbs & 90° wrap angle (wet-to-dry, room temperature).

In the final 5 trials the stiction peak was still visible; however, the kinetic COF value was observed to be steadily increasing. Figure 4.10 and 4.11 shows the results from the last 2 trials of the final phase of wet-to-dry experiments. The stiction values have not changed significantly, but the kinetic COF values point to a steadily increasingly drier interface. Trials 11-14 show a stiction peak value of 0.95, but the post stiction COF does not level off, instead it steadily climbs to as high as 1.4. All three trials had to be terminated before the kinetic COF could stabilize since the test setup was vibrating violently by this point. Due to the termination of the trials mid way, the ends of the trials appear as stiction peaks when in fact they are not; the interface had not yet been given enough time to stabilize. Trial 15 (Fig. 4.11), while still exhibiting a stiction

peak, achieved a stable kinetic COF state unlike Trials 11-14. The final kinetic COF value stabilizes at 1.55, a slightly high value for a dry interface. A final trial was conducted nearly 12 hours from the end of Trial 15. The results from the final trial point to a totally dry interface, with no stiction being observed. However, the kinetic COF value is higher than what was observed in Figure 3.1 (previous test for a dry room temperature interface with the same dead load and wrap angle).

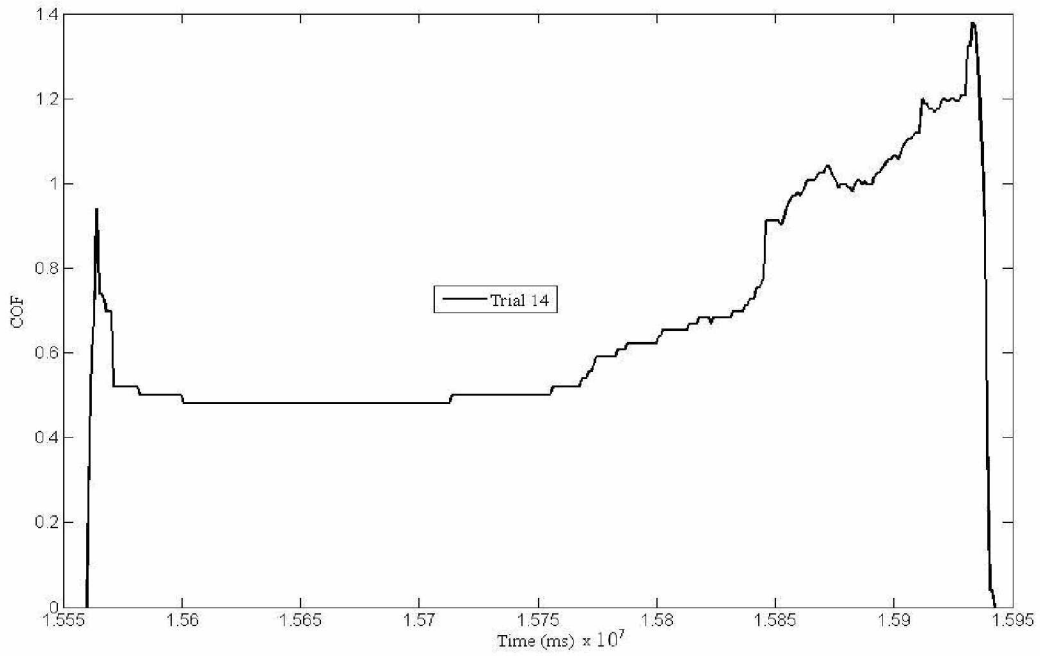

Figure 4.10 COF vs. Time for 2.5 lbs & 90° wrap angle (wet-to-dry, room temperature).

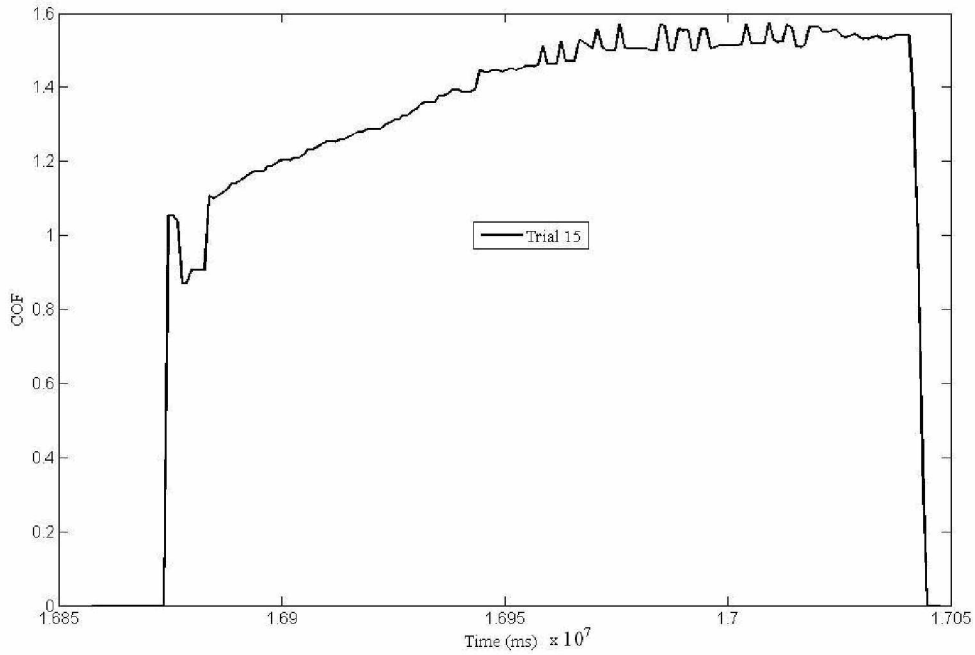

Figure 4.11 COF vs. Time for 2.5 lbs & 90^{o} wrap angle (wet-to-dry, room temperature).

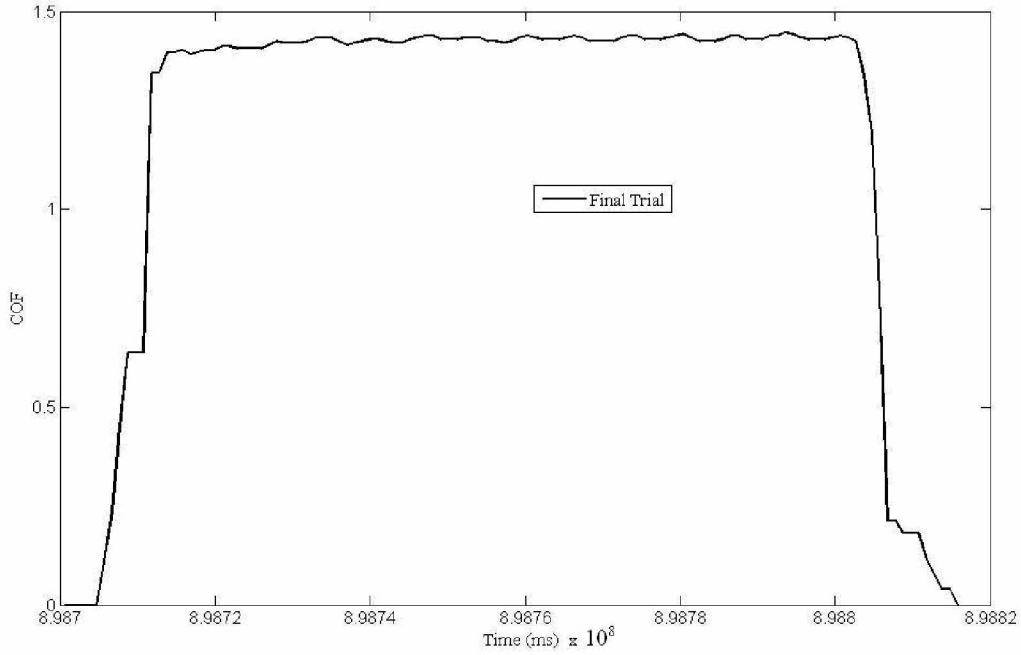

Figure 4.12 COF vs. Time for 2.5 lbs & 90^{o} wrap angle (wet-to-dry, room temperature).

4.4 Discussion

4.4.1 Wet Kinetic Friction

Previous research demonstrates that when rubber slides on a smooth, hard surface covered by water, the sliding friction is lower than dry friction [9, 10]. It is believed that when rubber slides on a hard surface covered by water, the water is trapped in the surface cavities of the hard surface, leading to reduced viscoelastic deformations of the rubber. Roberts investigated the water entrapment with slowly moving elastic surfaces [13]. He showed that the flexibility of the rubber surface leads to the entrapment of liquid by elastic deformations. In wet conditions, the mechanical properties of the vulcanized rubber were modified by liquid absorption. Mofidi et al. provide some understanding on the liquid entrapment phenomenon in the context of tire application [17]. The rubber friction on wet contact at low velocity is up to 30% lower than that on the corresponding dry surfaces. According to them, hydrodynamic effect may not be the reason for friction reduction; instead, water smoothes the substrate and reduces the major friction contribution due to induced viscoelastic deformations of the rubber by surface asperities. Koenen and Sanon discussed the friction of a rubber blade on glass with involved water [16]. They discussed the influence of velocity on the friction coefficient of a wiper's rubber blade under wet condition and the associated noise. The wet rubber blade-glass interface exhibits a friction due to both boundary lubrication and mixed lubrication.

In previous research works, high static friction of wet rubber has never been reported. In our studies, to account for the observed high static friction of wet rubber, we assume that wet rubber belt-pulley contact can be represented by Figure 4.13. Because of the trapped water, the interface could be flooded by water to form a water pool (Fig. 4.13a), or it could be wetted with water film and leave some cavities in the deep valley regions (Fig. 4.13b). In comparison, a dry interface is represented in Figure 3.10. For the measured wet kinetic friction shown in Figures 4.1-5, the trend is quite different from previously published results of water-lubricated rubber in which both boundary and mixed lubricated regions exist. In previously published research, the wet rubber frictions have negative slopes in the friction vs. velocity curve [6, 13-17]. However, Figures 4.1-5 show that the wet kinetic friction remains almost constant in most of the test speed range (the upper limit is 0.87 m/s). This observation is valid for all of the belts tested.

Another unique aspect of the current research is the two different acceleration conditions used in the testing phases, which have not been studied or tested before. However, our studies could not satisfactorily explain the different kinetic COF values observed for the two acceleration conditions (i.e., higher kinetic COF for slow acceleration compared to quick acceleration).

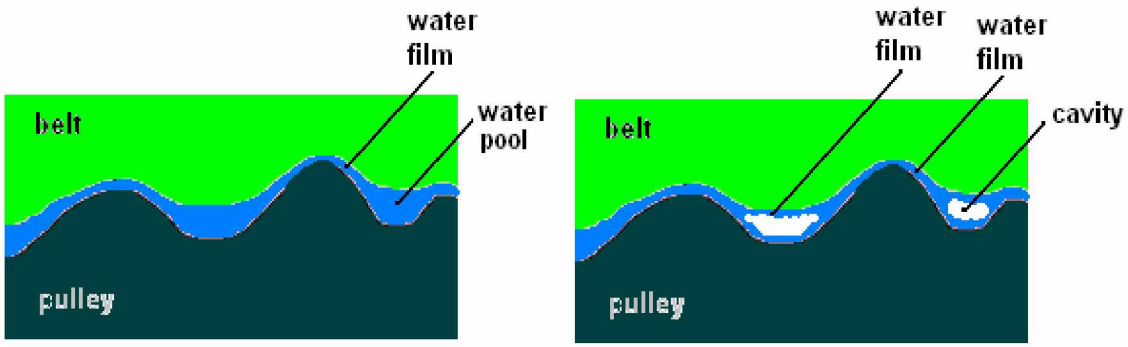

(a) Flooded with water pools (b) with cavity

Figure 4.13 Schematic of wet rubber belt contact with pulley surface.

4.4.2 Wet Static Friction

The schematic of a wet rubber belt on a pulley surface is shown in Figures 4.13 and 4.14. If the entrapped water is sufficient to fill all cavities in the interface, then it can be represented by Figure 4.13a. If the entrapped water is only sufficient to wet the whole surface and leaves some cavities, then the case can be represented by Figure 4.13b. If there is only a small amount of water in the interface forming a surface film and water bridge, then the situation can be represented by Figure 4.14.

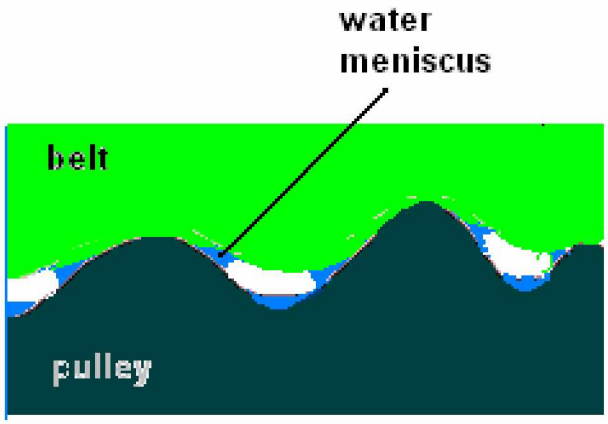

Figure 4.14 Schematic of rubber belt on a hard pulley surface with meniscus water bridge.

During contact, if water is introduced close to the region where the rubber completely follows the short-wavelength surface roughness profile of the pulley, surface tension results in a pressure difference across the meniscus surface referred to as capillary pressure. The pressure difference inside the meniscus, results in an intrinsic attractive force, called the meniscus force, acting on the interfaces. For hydrophobic surfaces, a repulsive meniscus force will act. When separation of two surfaces is required, the viscosity of the liquid causes an additional attractive force, rate-dependent viscous force during separation [18]. Meniscus and viscous forces govern the break of a meniscus bridge. The attractive force for a sphere in contact with a plane surface is proportional to the sphere radius R. For either the flooded case or water bridged case, the adhesion developed due to capillary effect could be significant. If the adhesion pressure is close to the order of magnitude of normal pressure, it could have a substantial effect on the friction of the belt. We can estimate the adhesive force

developed due to capillary effects based on established formulations [18-24]. The resultant force, adhesive or repulsive, is highly dependent on the formed meniscus area, contact angles, number of menisci, separation time, and surface tension and viscosity of the liquid. Consider that at the peak of the pulley asperity region, the rubber completely follows the short-wavelength surface roughness profile of the pulley. The contact asperities wetted by the water film contribute to the total meniscus force. In general, given the mean peak radius R (asperity radius), the surface tension of water γ, water film thickness h, and the number of summits per unit area N, the macro-meniscus force can be solved. The meniscus force is given by:

$$F_m = f_m AN \tag{4.1}$$

in which A is the apparent contact area, f_m is the meniscus force per asperity.

The capillary force assumes a maximum value when all of the interfacial cavities are completely filled with water. For simplification, if water is flooded (Fig. 4.13a), we have

$$f_m = 2A_m \gamma(\cos\phi)/h \tag{4.2}$$

where A_m is the asperity area projected on to the meniscus surface, and ϕ is the contact angle between water and rubber surface.

For water bridged asperity (Fig. 4.14), the meniscus force per asperity is

$$f_m = 4\pi R\gamma(\cos\phi) \tag{4.3}$$

The total tangential friction force can be estimated by

$$F_T = \mu_s(F_n + F_m) + F_v \tag{4.4}$$

where μ_s is the static friction coefficient, F_n the normal/applied operation load, and F_v the viscous shear force. Figure 4.15 shows the relation between adhesion pressure/contact pressure ratio with water thickness for a water mediated interface. From Figure 4.15 we can see that the water adhesion increases rapidly with respect to normal/contact pressure when the interface separation or water film thickness is reduced. When the separation is less than 3 micrometers, the adhesion pressure exceeds the normal/contact pressure from tension load. This leads to extra static friction force and allows the static friction force to be substantially higher than in the dry condition.

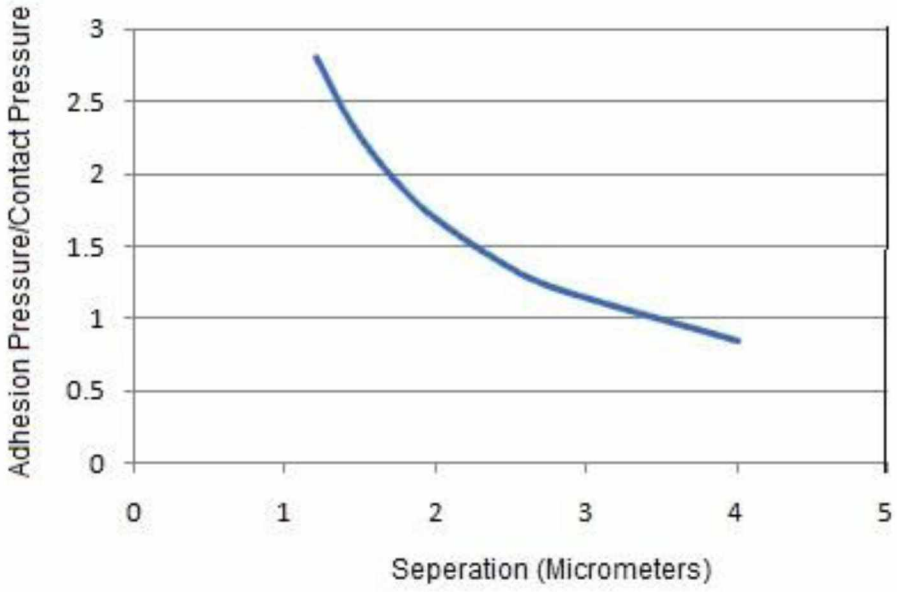

Figure 4.15 Relation between adhesion pressure/contact pressure ratio with water thickness for belt-pulley interface.

However, in Equation 4.4, it is assumed that μ_s is constant as F_m changes, which is not necessarily true. The relation between μ_s and F_m is not known. Equation 4.4 only

partially explains the higher value of static COF. Also, we could not explain the difference in the kinetic COF values for quick and slow acceleration conditions. Once again, as with kinetic COF, higher stiction is observed in slow acceleration trials compared with quick acceleration trials (Figs. 4.3-4.5). One explanation of this could be the different shear rates in the two conditions. As mentioned earlier, the force required to separate the contact surfaces is time dependent. Higher/quick acceleration implies a higher shear rate and lower than low/slow acceleration, which tends to overcome the adhesive forces of the trapped water more quickly and easily in the former than in the latter case. However, this is not a definite theory, just a possible explanation based on observing the results. Future prospects for this study could include a detailed study on the variation in static and kinetic COF values in wet testing for different acceleration conditions.

4.4.3 Wet-to-Dry Friction

As mentioned in Section 4.4.1, the wet kinetic friction remains almost constant in most of the test speed range. Also, for the first 10 trials in the wet-to-dry case, the same trend repeats; and then the wet kinetic friction abruptly jumps to the dry friction level or even higher in certain threshold runs (typically 9-12 runs). This suggests that the belt-pulley interfaces in start-up running are basically dominated by boundary lubrication and that the very thin water film needed for boundary lubrication is sustainable up to about ten runs, then it disappears abruptly.

Unlike reported belt testing results based on the SAE test rig where water is continuously supplied [1,6] when the belt is under coast-down running from high speed, in the current test, water is fully sprayed to the interface only before start-up test running. Each start-up test run lasts from 5 to 20 seconds. The start-up testing can run consecutively up to ten times with almost identical results before the wet kinetic friction abruptly jumps to a high level due to complete dry-up. It is natural to assume that the evolution of the wet interface is from the status shown in Figure 4.13a to the status shown in Figure 4.13b, due to water evaporation, squeeze-off, or spin-off in consecutive start-up running. Based on this assumption of the evolution of interfacial water, and in view of the constant kinetic wet friction vs. speed, it can be inferred that the wet kinetic friction is dominated by the surface water film instead of by the amount of entrapped water. The sorption of film on the surface plays a key role in friction. The abundant water in the pool of the valley seems only to have the function of supplying water to the film to maintain running until all water is exhausted. If the extra entrapment water (in the pool besides film) contributes to friction, then friction will be affected in the consecutive running by the decreasing amount of water; however, results show that kinetic wet friction remains the same until a sudden jump to dry friction in a threshold run. This suggests that the water sealing effect or water smoothing effect [14] is not a strong factor for the wet belt friction seen in our results, as the sealing effect is proportional to the amount of water entrapped in the interface. According to boundary lubrication theory, the film could consist of a very small monomolecular layer; in other words, it needs only a very small amount of water to attain wet kinetic friction. Test

results show that the water entrapment capability is not strong for the belt-pulley interface, sustaining about ten runs. Moreover, the water squeeze-off effect is not strong, in contrast with previous research of rubber for different applications [15]. The progressive process of water squeeze-off in the rubber contact area reported by Persson and Mugele [15] does not occur in the belt pulley interface; instead, the water film of the whole belt interface is dependent on the amount of entrapped water and abruptly vanishes in certain threshold runs when the belt is under consecutive start-up running.

The experiment pointed to an increasing kinetic COF - to values even greater than normal dry kinetic COF - in the final phase, similar to what was observed by Koenen and Sanon [16] in a rubber-glass interface. The glass surface in this situation is called tacky glass. Though no explanation could be given (in this research or in Koenen's), they prescribed a few possible solutions to decrease COF, surface treatment or coating modifications of the glass surface. Further research could explain why the kinetic COF exceeded values from a completely dry interface.

4.5 Conclusion

This chapter presented experimental characterization and analysis of friction of wet belts based on the belt-pulley test rig. It quantifies the effects of wet conditions on friction and sound during start-up running. Its main conclusions are as follows: the static frictions under wet contact are higher than the wet kinetic friction force by 40%-60% subject to different kinds of belts, due to water capillary effect. The wet static friction is

also higher than the dry static friction. The wet kinetic friction is lower than the dry kinetic friction by about 30%-40%. The wet kinetic frictions are basically dominated by boundary lubrication. The very thin water film slightly changes the surface adhesion. The involved water film in start-up running is too thin to form mixed lubrication. The wet kinetic friction remains almost constant with increasing speed range.

When a wet belt is under consecutive start-up running, the water pools in interface valleys can supply water to the surface to maintain the existence of water film, thus forming a dynamic equilibrium of film to yield a constant kinetic friction for different runs. This process continues until the total water amount in the interface reaches a certain minimum threshold of about ten runs (during this process, the amount of water is being continuously reduced by squeeze off, spin off, or evaporation). After the threshold run, the friction abruptly jumps to a high level of dry friction. The mechanism of jump remains open for further study.

CHAPTER 5

COLD FRICTION

5.1 Introduction

The friction of rubber under cold condition is extremely significant to safety and performance of vehicles and machines in cold climates. While rubber is regarded as having especially good friction properties under room temperature, it has a higher coefficient of friction under low temperature. Over the last decade, the reliability and durability performance of engineering rubber materials has substantially improved due to progress in materials science and engineering. In the automotive rubber industry, a big portion of the research and development budget has been spent addressing issues of friction and noise of components and systems.

Almost all kinds of accessory belts used in automotive engine systems have no cover. These belts are located close to the road surface, exposed to ambient conditions; hence the belts are susceptible to environmental effects. The presence of water or snow on belts is unavoidable during rainy or cold conditions. This water or snow usually induces water film in the rubber belt-pulley interface. Under low temperatures, this water film could convert into an ice film that changes the interface friction in the next cold-start running. In practical applications, start-up running with improper friction often causes belt and pulley noise. Published experimental results show that wet belt slip

could induce noise in some applications. Meckstroth and Ahoor [2] studied the tribological and dynamic properties of belts under dry and wet conditions. The widely used SAE Standard J2432 [7] defines the test procedure to characterize slip friction of belts under dry and wet conditions. However, the SAE J2432 [7] procedure does not define cold start-up running for testing. In cold start-up operation, the interface is under the cold condition only at the beginning. The larger static friction in start-up was only hypothesized as a possibility; it was not observed by using an SAE test rig. There has been a lack of research characterizing and quantifying cold belt static friction and the associated noise in start-up running. It is widely realized that many belts develop a noise problem during cold start-up running and that this kind of cold friction noise persists for a short period only and dies away after the system dries. Since this type of phenomena directly affects customer perception of product quality and causes warranty cost, it has received wide attention. When belts are used in snowy situations or in wet and cold situations, the belt-pulley interface is likely to form ice film. An ice-mediated interface involves more complicated physical mechanisms. One such complication is the adhesion and plastic deformation of ice at the friction interface which works at very low velocities before break up of the ice film. Another is the ice or water lubrication mechanism working at sliding velocities at relatively higher speed.

This chapter is aimed to provide an experimental characterization and analysis of friction of rubber belts under cold conditions. The motivation is to understand the friction and dynamics properties of commercially available ribbed rubber belts under cold start-up running, and to fill a void in the existing literature based on conventional

SAE Standard J2432 [7]. The ice adhesion effect and other effects are discussed and used to interpret the effects of pertinent parameters on the static and kinetic friction forces and to correlate with the experimental results. This study provides accessory drive designers some fundamental understanding of belt start-up friction under varied cold conditions.

5.2 Friction of Belt without Ice Film

Figures 5.1-5.3 are the graphical representation of the measured COF at 90^{o} wrap angle under dry-cold (-20^{o}C) conditions for 5 lbs, 2.5 lbs, and 10 lbs dead load, respectively. Relative humidity levels during the cold testing phase (Nov 2009 – Jan 2010) fluctuated between 50% and 65%. However, the winters in Fairbanks are considered dry. In Figure 5.1 the original force acting on the belt is 5 lbs due to dead load. When the pulley is driven to rotate, it applies a friction force on the belt, which causes an increase of the tangential force of the belt. Once again, it is noted that this work does not aim at an extensive investigation to get the best results of certain sample for optimal design. The emphasis is instead on describing and interpreting the general friction behavior, pointing out trends and the related vibration properties for future investigations, modeling and, development.

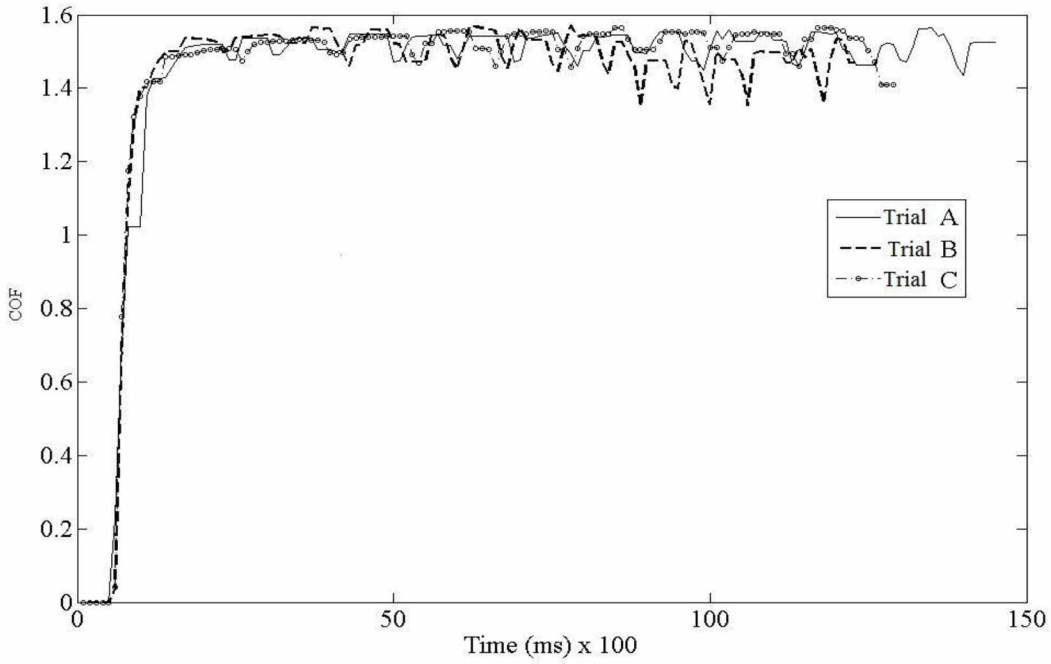

Figure 5.1 COF vs. Time for 5 lbs load & 90^{o} wrap angle (dry, cold -20^{o}C conditions).

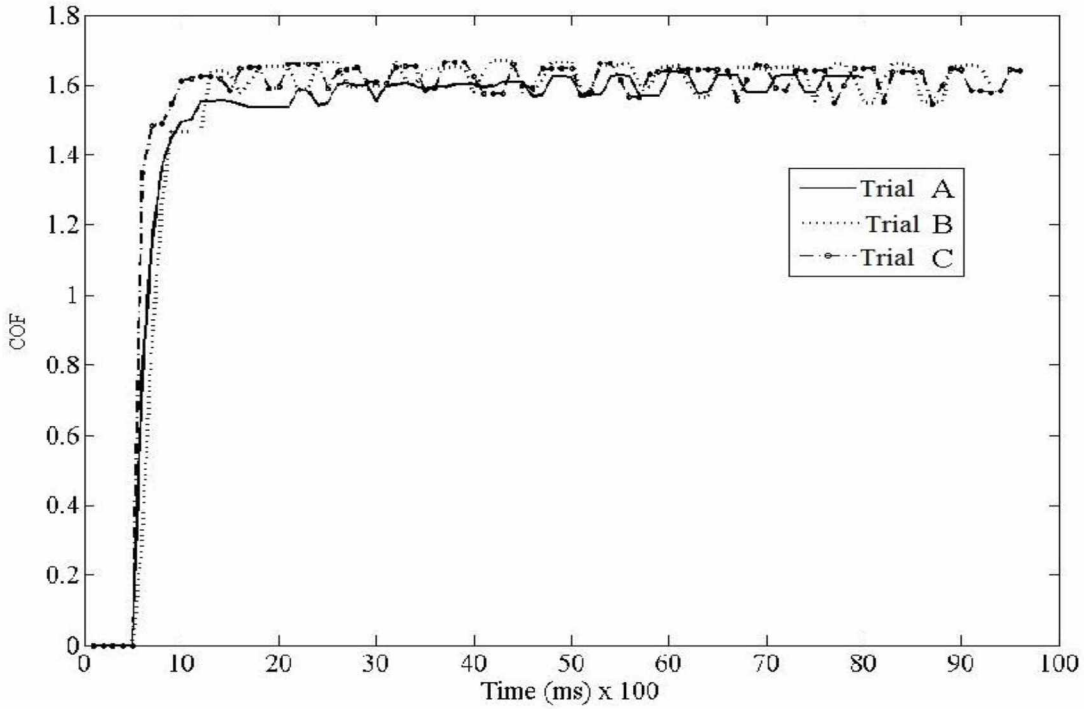

Figure 5.2 COF vs. Time for 2.5 lbs load & 90° wrap angle (dry, cold -20°C conditions).

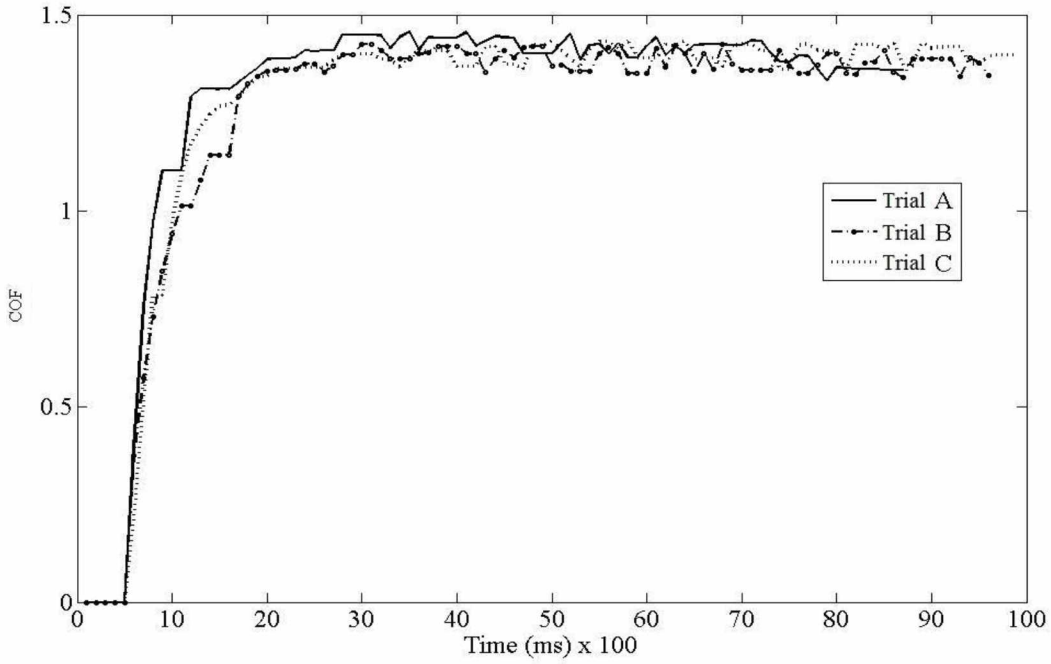

Figure 5.3 COF vs. Time for 10 lbs load & 90^{o} wrap angle (dry, cold -20^{o}C conditions).

Comparison of the results in Figures 5.1-3 with results in Figures 3.1, 3.4 and 3.15, shows kinetic COF under dry-cold conditions (for similar load and wrap angles) to be significantly higher than COF at dry-room temperature.

5.3 Friction of Belt with Ice Film

The belt-pulley interface is next tested for the frozen condition (wet interface under cold conditions). Both the belt and the pulley are wet and are immediately brought into contact with each other. The appropriate loads are applied and the interface is allowed to cool down to the surrounding ambient temperature of around -20°C (the whole process takes about 45 seconds), giving enough time for the water in the interface to freeze. The testing procedure is then followed for the rest of the testing conditions (Section 2.4). Figures 5.4 - 5.6 show the recorded COF in start-up running for wet cold conditions for different dead loads. As was done for wet-room temperature tests, the trials for wet-cold temperature tests are divided into slow and quick acceleration trials. In Figure 5.4, Trials A and C are quick acceleration trials while Trial C is a slow acceleration trial. The results follow the same trend seen in wet-room temperature trials – quick acceleration trials show a smaller peak in the graphs compared to slow acceleration trials. The peaks in this case, however, are not due to stiction, but rather to the adhesion properties of ice in the interface. Another notable difference between wet-room temperature results and wet-cold temperature results is that while the peak values are higher in wet-cold conditions, the kinetic COF is higher in wet-room temperature conditions. Thus, the difference between peak values and kinetic COF values is very large in wet-cold temperature (almost 1700%-1900%) compared to wet-room temperature conditions (40%-60%).

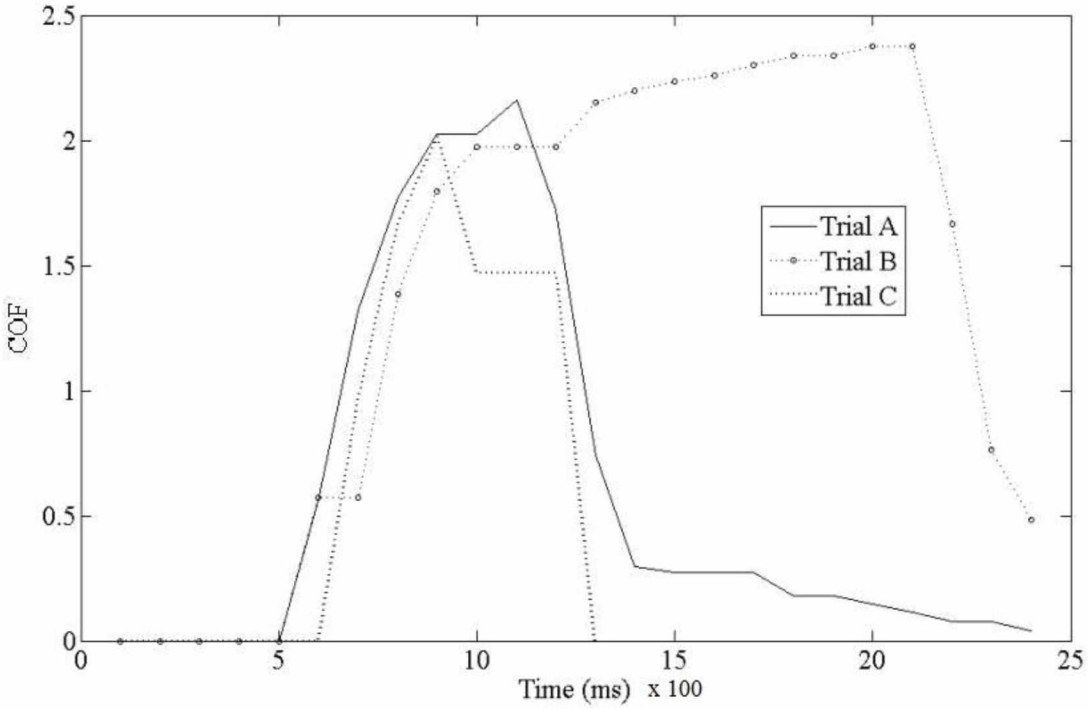

Figure 5.4 COF vs. Time for 2.5 lbs load & 90° wrap angle (wet, cold -20°C conditions).

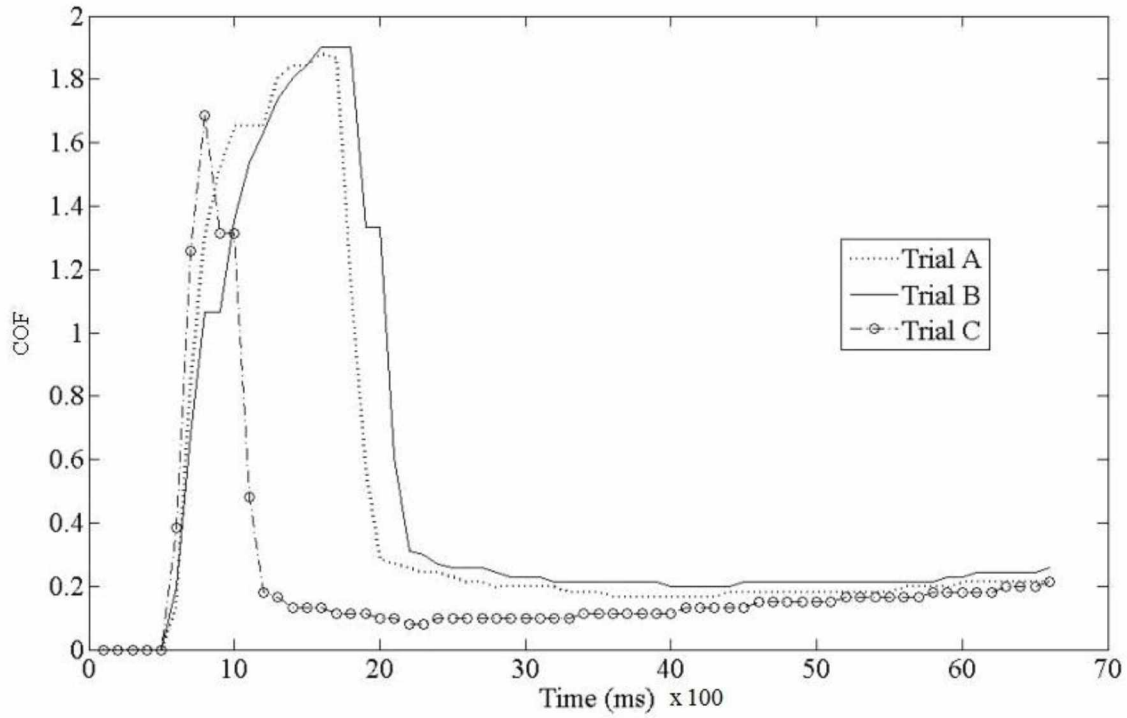

Figure 5.5 COF vs. Time for 5 lbs load & 90^{o} wrap angle (wet, cold -20^{o}C conditions).

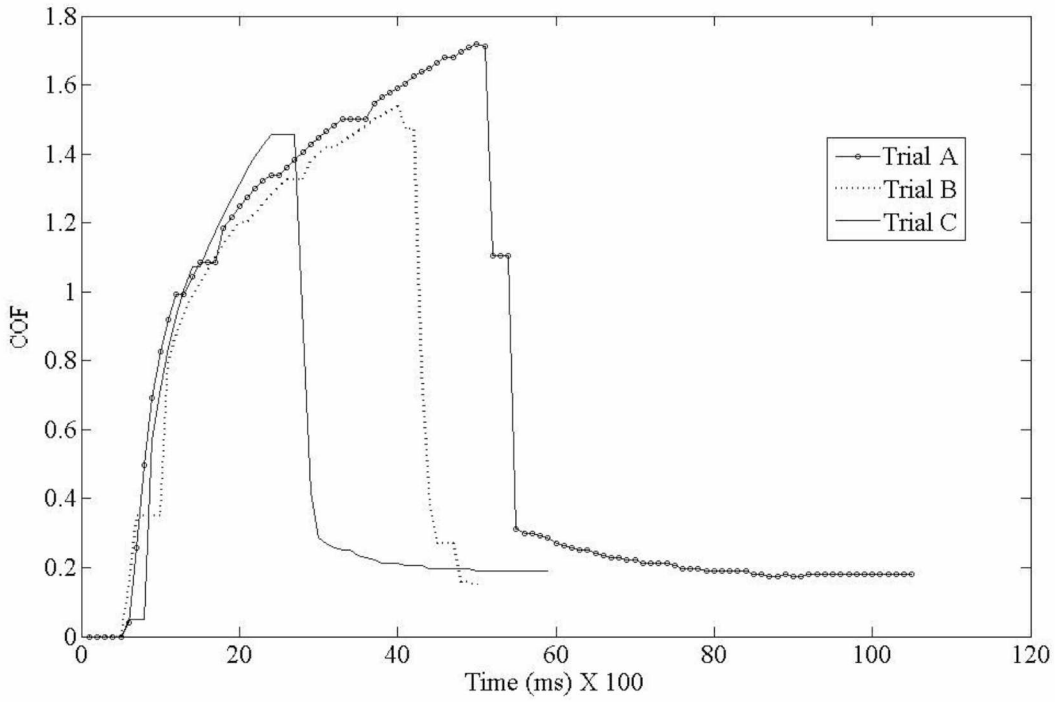

Figure 5.6 COF vs. Time for 10 lbs load & 90^{o} wrap angle (wet, cold -20^{o}C conditions).

Note that, unlike in wet-room temperature tests, here the difference in the peaks between slow and quick acceleration is very small, and there is almost no difference in their kinetic COF.

(a) Before

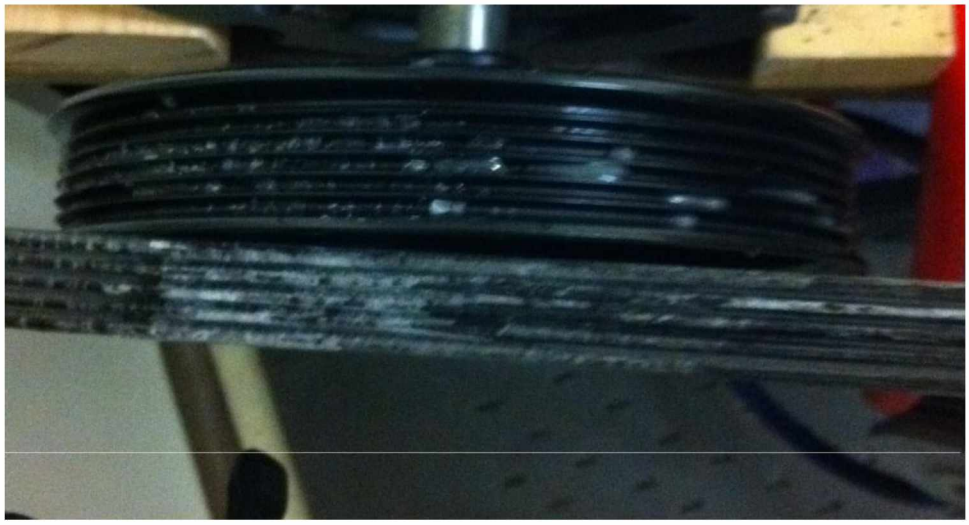

(b) After

Figure 5.7 Belt-Pulley interface (a) before being wet for a cold temperature test (b) after a wet-cold temperature test.

5.4 Discussion

5.4.1 Dry-Cold Friction

Comparison of the results found in dry-room temperature tests (Figs. 3.1, 3.4 & 3.5) with those of dry-cold temperature (Figs. 5.1-5.3), for the same dead load and wrap angle, shows that the COF under cold conditions is higher than that in room temperature conditions by 10%-20%.

As a fully viscoelastic frictional material, rubber has been investigated from a friction point of view [7, 12, 14, 15]. Dry friction under room temperatures has been discussed in detail in Chapter 3 (Section 3.5). As mentioned earlier, when rubber is in contact with a hard surface, rubber can deform elastically to establish an actual area of contact that is equal to the nominal area of contact for large contact pressures and a relatively smooth surface. A model of the adhesive friction of dry rubber is given in Equation 3.1. By comparing Figures 5.1-5.3, one notices, that belt friction increases slightly as load is progressively reduced from 10 lbs to 2.5 lbs, as would be expected from Equation 3.1.

To elaborate on the temperature dependence, we re-plot the results given by Higgins et al. [25] in Figure 5.8, which shows the property of rubber materials under different temperatures. The damping of polymer material is susceptible to temperature, as illustrated in Figure 5.8. In the very low temperature region, the material exhibits glass state. In this region, both Young's modulus E and shear modulus are high, but

material damping loss factor is low. In the low temperature region, Young's modulus E and shear modulus start to drop; material damping loss factor increases and attains its maximum. In higher temperature, Young's modulus E, shear modulus, and material damping loss factor decrease. High friction at temperatures around -20°C was caused by the internal friction associated with the rubber glass transition. From Figure 5.8 we can see that $\tan\delta$ decreases with temperature in the -20°C toward 20°C range. Thus Equation 3.1 suggests that belt COF increases with the decrease of temperature. This explains why the COF under cold conditions is higher than that in room temperature by 10%-20% observed above. However, the measured belt friction difference between room temperature and cold temperature (10%-15%) is not so salient as suggested by Figure 5.8 (100% difference of $\tan\delta$ between -20°C and 20°C); this could be explained by the fact that many other factors influence COF, and the effect of adhesion could take a dominant role instead of internal damping from slider body.

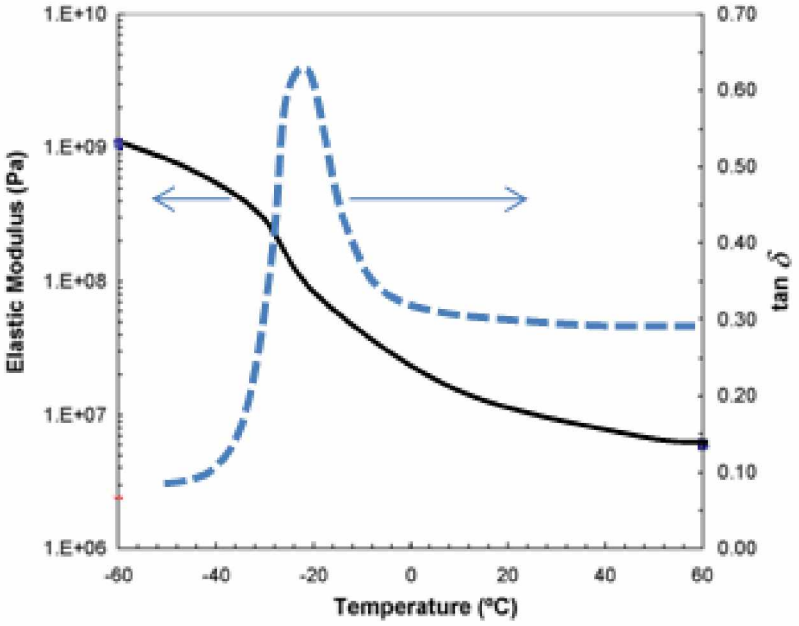

Figure 5.8 Property of rubber materials [25]

5.4.2 Cold Friction with Ice Film

Comparing Figures 5.4-5.6 with Figures 5.1-5.3, we can see that the wet-cold friction of a belt is substantially different from one in dry-cold condition. The wet-cold friction of the belt exhibits large static friction during the early phase of start-up running and exhibits very little kinetic friction at relatively high speed. The difference between static friction and kinetic friction is up to 1000%. Comparing Figure 5.3 with Figure 5.4 we can see that the static friction under lower load is higher than the case under higher load by 20%.

Obviously, the belt's wet-cold friction property is dominated by the formed ice film in the interface. The coefficient of friction of the interface with ice depends on many factors, such as asperities, temperature, sliding speed, normal load, and type of material. There are several possible physical phenomena involved: failure of ice film, pressure melting, and friction melting of ice film. In the literature [25-31], there have been documents of many observations concerning major factors affecting ice friction. The coefficient of friction of a material on ice decreases linearly as speed increases. Ice is one of the most slippery materials as its friction coefficient often becomes as low as 0.01 or even lower at certain high speed. The low friction property of ice is generally explained by two physical mechanisms which work at two different regions of sliding velocity: one is the water lubrication mechanism working at sliding velocities above roughly 0.01 m/s, and the other is the adhesion and plastic deformation of ice at the friction interface, which works at velocities lower than roughly 0.01 m/s. The coefficient of friction on ice could be as high as 0.3-0.9 depending on the materials involved when the sliding speed is very low. Adhesion occurs where there is no melting of ice at low speeds. It should be noted that when ice film is under mechanical stress, it could fail or delaminate from the friction pair surface.

To account for the observed high static friction of ice rubber, we assume that ice-mediated belt-pulley contact can be schematically represented by Figure 5.9. Before freezing and due to trapped water, the interface could be fully flooded or flooded in cavities between belt and pulley.

After freezing, the interface water could form a full ice film (Fig. 5.9a), or form micro ice body filling in the cavities (Fig. 5.9b). As shown in Figures 5.4-5.6, belt friction exhibits a large static friction and then abruptly drops to kinetic friction with the level much lower than the dry friction level. This suggests that the belt-pulley interfaces in start-up running are basically dominated by ice film lubrication. From experiments, the ice kinetic friction is much smaller than both the wet-cold static friction and the dry static friction. The sorption of water film on the surface plays a key role in the wet-cold friction. The water squeeze-off effect due to load effect is not very strong, but a higher load leads to slightly more water squeeze-off and accordingly less ice film formed and accordingly smaller frictions. The ice film of the whole belt interface is dependent on the amount of entrapped water, which is in turn dependent on the load effect, as illustrated in Figures 5.4-5.6.

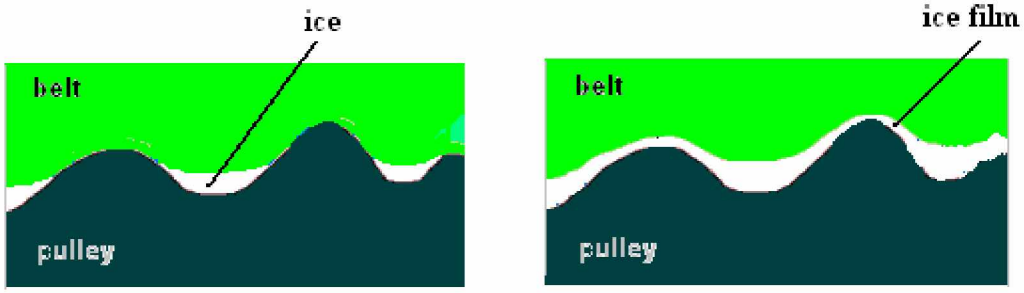

(b) Cavity filled with ice (b) Interface filled with ice film

Figure 5.9 Schematic of ice mediated rubber belt on a pulley surface.

Based on Figures 5.3-5.6 we can figure out the shear strength of the ice film in terms of the formula,

$$p = A / P \tag{5.1}$$

in which A is contact area and P is load.

According to static friction breakage data, the shear strength estimated by using the parameters in Table 2.1 is in the 0.05-0.15 MPa range. This range is smaller than the conventional reported ice shear strength, which ranges between 500 kPa and 900 kPa [26, 31-35]. This could be due to problems associated with generating a stress condition that corresponds to the assumed condition when analyzing the test results. Ice can strongly adhere to just about everything, including hydrophobic material. If water is frozen onto a clean metal surface, the interface is stronger than the ice and fracture occurs within the ice itself. The detailed behavior depends on the stresses developed near the interface. Surface contaminants on metal or rubber could reduce adhesion by a very large factor, and it is suggested that this is due primarily to a reduction in the area over which strong metal/ice adhesion occurs. On the other hand, the adhesion of ice to polymeric materials differs from the adhesion to metals. The interfacial strength appears to be less than the strength of ice, and failure occurs truly at the interface. Hydrophobic materials show very low adhesion to ice. The exact physical mechanisms of bonding between ice and other solids, the structure and properties of ice/solid interfaces, and the nature of ice adhesion are not very clear.

The reason for almost no difference in peak values between the slow and quick acceleration trials also could be that, unlike in wet-room temperature trials where we

hypothesized that the shear rate has a significant effect on stiction, the effect is not particularly visible in frozen interfaces. The ice shears impulsively, and the shear strength range for the ice film is 0.05-0.15 MPa (from Table 2.1). This range is not large enough to show any significant difference between quick and slow acceleration trials even considering that the two cases take up the two extremities of the shear strength range (i.e., quick acceleration shears ice at 0.05 MPa while slow acceleration shears at 0.15 MPa).

5.5 Conclusion

The purpose of the study presented in this chapter was to measure the friction between rubber belts and the pulley under cold conditions. This chapter has presented an experimental characterization and analysis of friction of cold belts based on a belt-pulley test rig. It allows the effects of cold conditions on friction and dynamics during start-up running to be quantified. The most significant conclusions for the assessment of the rubber belts under cold conditions are as follows:

- The friction coefficients measured under dry and cold conditions are higher than those at room temperature conditions, but the difference is not significant due to strong surface effects.
- The static friction coefficients measured under wet and cold conditions are significantly higher than those at room temperature conditions due to adhesion

effects. The estimated shear strength of ice film is in the 0.05MPa-0.15MPa range.

- The breakage process of static friction of rubber under wet and cold conditions is an impulsive process.
- The kinetic friction coefficients measured under wet and cold conditions is significantly lower that in room temperature, due to the melting film lubrications.

CHAPTER 6

NOISE ANALYSIS

6.1 Introduction

This chapter presents an experimental study of automotive v-ribbed belt slip noise under varying conditions. With a self-developed test setup, in this study a set of experiments were conducted to investigate the properties of belt noise due to friction. This study provides accessory drive designers with some fundamental understanding of belt startup noise under varying atmospheric conditions.

Automotive multiple v-ribbed belts are a key for transmitting power from engine crankshaft to automotive accessories. With improvement in quietness of vehicles, it is necessary to reduce the belt noise for higher quality vehicles. The endless industry emphasis on improving vehicle noise characteristics has resulted in a variety of new belt products intended specifically to inhibit friction-induced vibration and noise. Tighter controls over critical belt drive parameters have helped diminish the occurrence of objectionable belt vibration and noise. These include complex friction materials (composition, geometry), belt construction, drive system dynamics, components and integration, boundary conditions at the friction interface, all of which are subject to temperature and humidity variations, manufacturing and assembly tolerances, wear, non-linearity, and viscoelasticity. Some papers are dedicated to analysis of noise and

non-linear belt vibrations. Some published papers deal with linear and non-linear transverse/longitudinal belt vibration responses [36, 37]. The authors discussed models available for analyzing the free and forced axial, transverse, and tensional vibrations of belts. The effects of initial tension, transport velocity, bending rigidity, support flexibility, large displacement, and belt and pulley imperfections discussed. Connell and Rorrer [3, 38] systematically investigated friction-induced vibration and noise of v-ribbed belts. They characterized basic noise properties by extensive experiments. Dalgarno et al. [4] discussed the tangential slip noise of v-ribbed belts and attributed the noise to the excitation of the fundamental vibration of belts. Based on the experiments using an SAE test rig, researchers presented mathematical models that unified previous works [5, 39]. Cold startup noise has been one of the critical issues of v-ribbed belts in applications. A typical accessory system consists of a transmission belt, crankshaft pulley, tensioner pulley, idler pulley, air conditioning pulley, compressor pulley, power steering pump pulley, alternator pulley, and water pump pulley. All accessory pulleys are driven by the belt. When the load torque of some accessory is beyond the belt driving torque on its pulley, belt tangential slippage on the pulley will occur. Intermittent slip noise, “chirp” or “squeak” will occur if friction and slip reach a threshold level [3-5, 38, and 39]. However, slip noise and friction of the belt under certain application conditions such as cold start and overload under cold conditions have not been addressed.

The noise testing is conducted on a belt-pulley test setup at both room temperature and cold temperature. Belt noise is recorded when the belt is forced to a slip motion under varied conditions. The experimental procedure is described in Section 2.4.

6.2 Dry-Room Temperature Noise

The waveform and spectrogram of the slip noise under room condition is shown in Figure 6.1. The squeal noise has a quite low frequency of 3.5 kHz and its harmonics of 7 kHz. Moreover, the recorded accelerations are consistent with the waveform and spectrogram of noise. To correlate with recorded noise, the interface frictions are also measured. The measured effective coefficient of friction (effective COF, including the wedge action of v-rib) while the pulley is rotating from zero to specific rpm is shown in Figure 3.4.

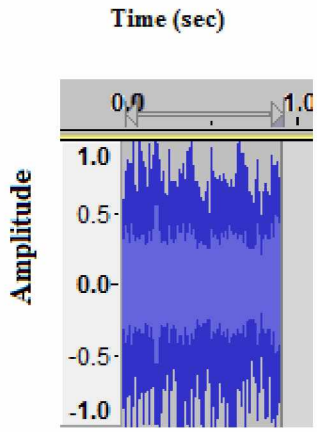

(a) Noise Waveform

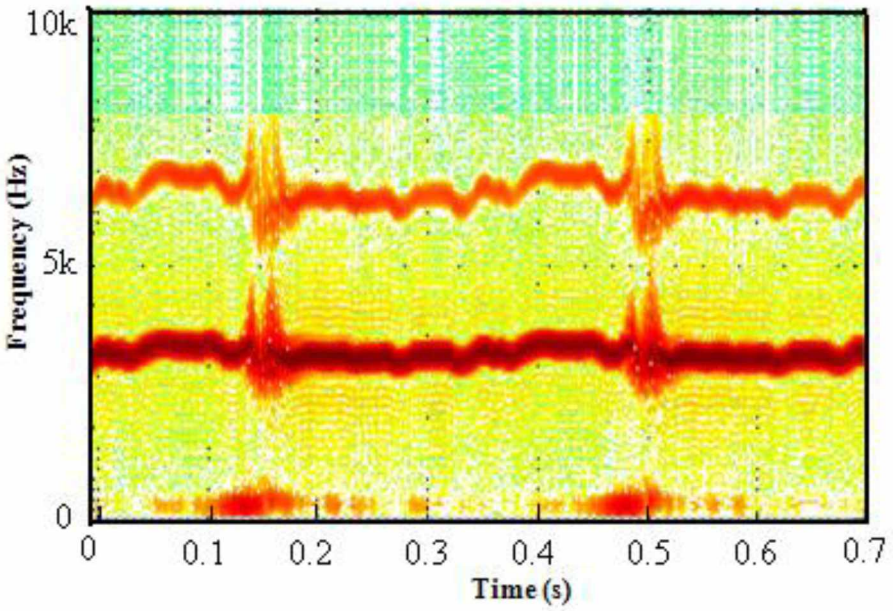

(b) Spectrogram

Figure 6.1 Measured noise waveform and spectrogram for 5 lbs load & 90^{o} wrap angle (dry, room temperature).

Figure 6.2 shows the first natural mode of the belt rib of natural frequency of 3.1 kHz, obtained by using finite element analysis, which is likely to be excited in dry friction tests. This is consistent with results in Figure 6.1 and with previous studies [4, 38, and 39].

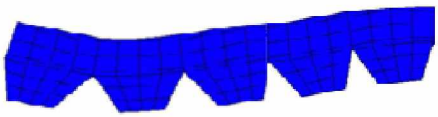

Figure 6.2 First natural mode of belt rib modeled by Finite Element Method.

6.3 Wet-Room Temperature Noise

Previous research works demonstrate that dry noise frequencies for belts are correlated with the natural modes. In this section, noise under wet-room temperature conditions is recorded and studied. The measured result in Figure 6.3 shows that the spectrum signature of sound in the breakage of wet static friction is of impulsive type with a frequency spectrum extending to 20 KHz followed by a wideband frequency pattern without having the salient component of a specific frequency. This suggests that the natural modes of the belt rib are not significantly excited in wet start-up running.

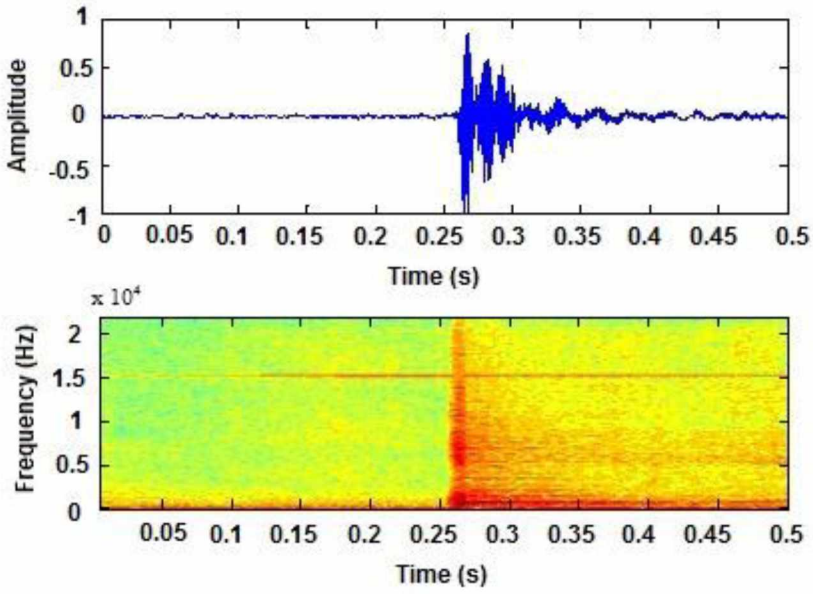

Figure 6.3 Measured noise waveform and spectrogram for 2.5 lbs load & 90° wrap angle (wet, room temperature).

6.4 Cold Noise

Figures 6.4 and 6.5 show the recorded noise waveform and spectrogram of typical slip noise waveform under dry-cold condition and wet-cold conditions, respectively. In Figure 6.4 the squeal noise has a high frequency of 9 kHz and harmonics of 18 kHz, whereas wet-cold noise, Figure 6.5, is an impulsive sound with a wideband spectrum. Previous research works demonstrate that dry belt noise frequencies for belts are correlated with the natural modes and harmonics of belt rib due to friction-induced instability of mode coupling or negative damping from a negative slope of the COF versus speed curve, and the specific frequency is in the range of 3-4 kHz [3, 4 and 6] and its harmonics (Fig. 6.1).

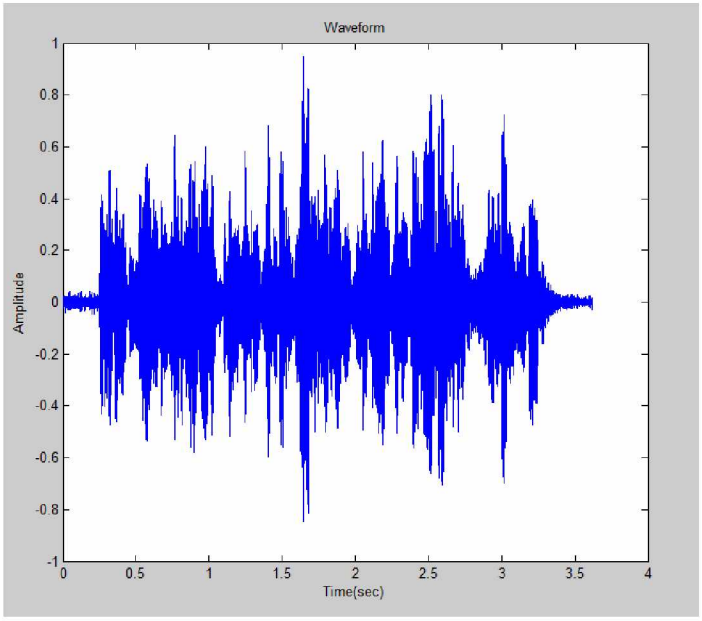

(a) Noise waveform

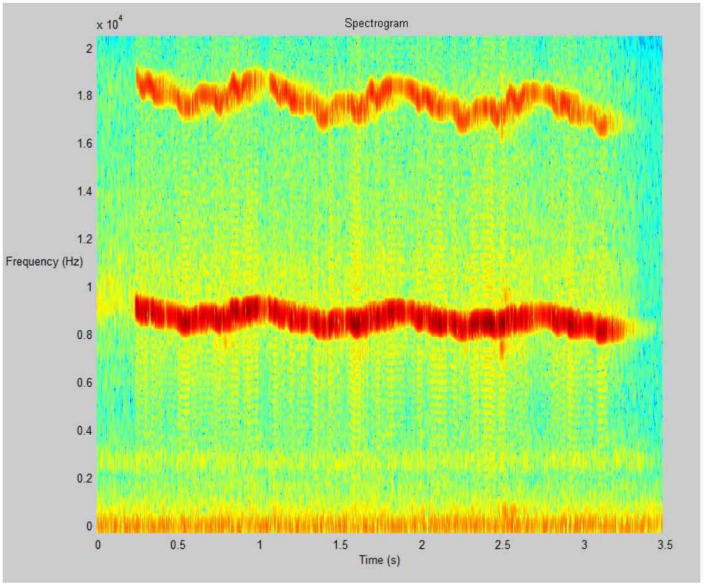

(b) Spectrogram

Figure 6.4 Measured noise waveform and spectrogram for 5 lbs load & 90^{o} wrap angle (dry, cold -20^{o}C conditions).

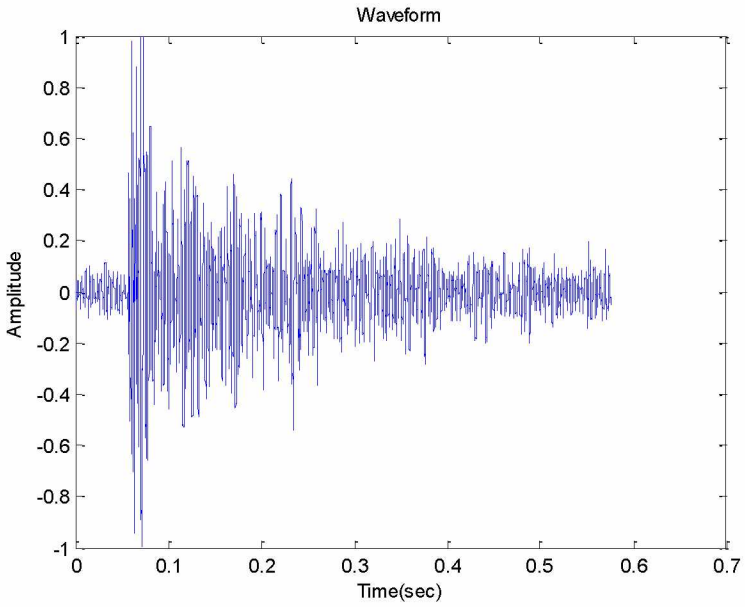

(a) Noise waveform.

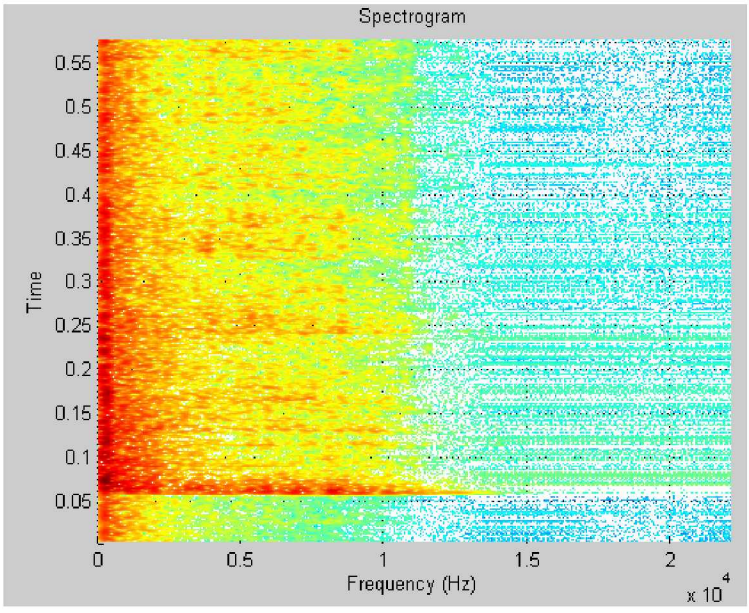

(b) Spectrogram

Figure 6.5 Measured noise waveform and spectrogram for 5 lbs load & 90^{o} wrap angle (wet, cold -20^{o}C conditions).

However, the measured result in Figure 6.4 shows that the noise associated with cold-dry start-up running has a specific frequency of 9 kHz and its harmonics of 18 kHz. The substantial difference in frequency could remarkably impact customer perception of belt noises under cold conditions and room temperature. On the other hand, the measured result in Figure 6.5 shows that the vibrations associated with wet-cold start-up running exhibit a wideband frequency pattern without having the salient component of a specific frequency. This suggests that the natural modes of the belt rib are not significantly excited in wet start-up running. As seen in the wet-room temperature result, Figure 6.3, the spectrum signature of sound in the breakage of wet static friction is of impulsive type.

6.5 Discussion

Figure 5.1 shows that belt friction under cold condition has a 15% higher value than that in room temperature condition (Fig. 3.4), which is not a substantial value. The COF profile under room temperature and cold temperature are similar. Since the belt friction under cold condition is similar to that under room temperature, and considering that the COF is the key factor influencing slip noise [3-5, 38, 39], we can assume that the mechanisms of belt noise under room temperature and cold condition are similar. Moreover, it is noted that the higher slip friction is more likely to cause friction noise. As such, the belt under cold condition could have slightly higher likelihood to generate noise than it would in room condition.

To interpret the much higher squeal frequency of belt noise under dry-cold condition, we can correlate this with rubber's elastic modulus change with respect to temperature. Figure 5.8 [25] illustrates rubber's elastic modulus as a function of temperature. It can be seen that the rubber's elastic modulus at cold temperatures (-20°C) is 10 times higher than that at room temperature (23°C). In view of that, the belt slip squeal noise frequency is correlated with the rib natural frequency [3-5, 38, 39]. If we assume the equivalent spring constant of the belt rib is k_{eq}, equivalent mass is m_{eq}, then the natural frequency of the rib is

$$f_{room} = \frac{1}{2\pi}\sqrt{\frac{k_{eq}}{m_{eq}}} \tag{6.1}$$

Under cold condition, if we have $k_{eq\_cold} = 10k_{eq}$, equivalent mass is m_{eq}

$$f_{cold} = \frac{1}{2\pi}\sqrt{\frac{k_{eq\_cold}}{m_{eq}}} = \frac{1}{2\pi}\sqrt{\frac{10k_{eq}}{m_{eq}}} = 3.3 f_{room} \tag{6.2}$$

Equation 6.2 suggests that the rib's natural frequency under cold temperature is 3.3 times higher than its value under room temperature. This observation is well correlated with the experimental results of Figures 3.4, 5.1, 6.1 and 6.4. It is noted that the substantial difference in frequency could remarkably impact the people's perceptions of belt noises under cold condition and room temperature.

6.6 Conclusion

This chapter presented an experimental investigation of automotive v-ribbed belt slip noise under various conditions. It was previously shown that belt friction under cold condition has higher value than that in room condition, but the difference is insubstantial and the friction profiles are similar. As such, we can hypothesize that the mechanisms of dry belt noise under room temperature and cold condition are similar. On the other hand, the belt noise under cold condition has much higher squeal frequency due to elevation of the elastic modulus of rubber under cold condition, which could remarkably impact the perception of cold noise. The noises recorded from the wet belt under both room temperature and cold temperature also exhibit similar properties between them. The noise is of impulsive type exhibiting a wide band spectrum. This study is expected to provide accessory drive designers some fundamental understanding of belt startup noise.

CHAPTER 7

CONCLUSION

An experimental test setup has been constructed for studying the friction properties of an automotive ribbed v belt-pulley system. Based on the results from the experiments conducted, the following conclusions can be deduced:

1. In terms of the results from dry-room temperature tests, the conventional theoretical model proposed in previous research work is valid for a dry rubber belt-pulley interface.

2. Results from wet-room temperature tests show that static friction is much higher than kinetic friction (by almost 40%-60%); wet kinetic friction is lower than dry kinetic friction; wet belt under consecutive start-up runs maintains the existence of water film (due to water supply from water pools) for a few runs, thereby exhibiting wet interface properties despite no introduction of additional water in the interface. After the threshold runs, the friction abruptly jumps to a high level of dry friction (possibly due to squeeze off, spin off, or evaporation).

3. Results from dry-cold temperature tests show that COF values are higher under cold temperatures than at room temperature for the same dead load and wrap angle.

4. Wet-cold temperature tests show that breakage of static friction of rubber under cold wet conditions is impulsive, and kinetic COF is significantly lower than for wet-room temperature.

5. Analysis of the noise results shows the mechanisms of dry belt noise under room temperature and cold condition to be similar, with noise under cold condition having higher squeal frequency; wet belt under both room temperature and cold temperature also exhibits similarities in noise; the noise is of impulsive type exhibiting a wide band spectrum.

REFERENCES

[1] Meckstroth, R. J., 1998, Accessory Drive Belt/Pulley Friction Test, SAE 980837.

[2] Ahoor, L. and Meckstroth, R. J., 1990, Belt Tracking Experiment, SAE Paper 901770.

[3] Connell, J.E. and Rorrer, R.A.L., 1992, Friction-induced vibration in v-ribbed belt applications, ASME DE-Vol. 49, 75-85.

[4] Dalgarno, K.W., Moore R.B. and Day, A. J., 1999, Tangential slip noise of V-ribbed belts, Proceedings of the Institution of Mechanical Engineers, Part C: Journal of Mechanical Engineering Science, 2041-2983, 741-749.

[5] Sheng, G., Liu, K.M., Otremba, J., Pang, J., Qatu, M. and Dukkipati, R., 2004, A model and experimental investigation of belt noise in automotive accessory belt drive system, International Journal of Vehicle Noise and Vibration, 1, 1-2, 68-82.

[6] Sheng, G., Miller, L. D., Brown L. and Otremba J., 2006, Wet belt friction-induced dynamic instability and noise in automotive accessory belt drive systems, Int. J. Vehicle Noise and Vibration, 2, 3, 249.

[7] SAE Standard J2432, 1998, Performance Testing of Pk Section v-ribbed Belts, SAE J2432 International.

[8] Pang, J., 2007, NVH of automotive power train, SAE China NVH conference, Beijing.

[9] Persson, B.N.J., 1998, On the theory of rubber friction, Surface Science Reports, 401, 445–454.

[10] Persson, B.N.J., 1999, Sliding friction, Surface Science Reports; 33, 83- 119.

[11] Myshkin, N.K., Petrokovets, M.I. and Kovalev, A.V., 2005, Tribology of polymers: Adhesion, friction, wear, and mass-transfer, Tribology International, 38, 910–921.

[12] Zhang, S.W., 1998, State-of-the-art of polymer tribology, Tribology International, 31(1–3), 49–60.

[13] Roberts, A.D., 1971, Squeeze film between rubber and glass. J Phys D: Appl Phys, 4, 423–34.

[14] Persson, B.N.J., Tartaglino, U., Albohr, O. and Tosatti, E., 2005, Rubber friction on wet and dry road surfaces, Phys Rev, B 71, 035428.

[15] Persson, B.N.J. and Mugele, F., 2004, Squeeze-out and wear: fundamental principles and applications, Journal of Physics: Condensed matter, 16, 295–355.

[16] Koenen, A. and Sanon, A., 2007, Tribological and vibroacoustic behavior of a contact between rubber and glass (application to wiper blade), Tribology International, 40, 1484–1491.

[17] Mofidi, M., Prakash, B., Persson, B.N.J and Albohr, O., 2008, Rubber friction on (apparently) smooth lubricated surfaces, Journal of physics, 20, 085223 (8pp).

[18] Cai, S. and Bhushan, B., 2007, Meniscus and viscous forces during normal separation of liquid-mediated contacts, Nanotechnology, 18, 465704.

[19] Bhushan, B. and Kotwal, C.A., 1998, Kinetic meniscus model for prediction of rest stiction, ASME Transactions of Tribology, 42, 120.

[20] Alexandre, C., 2007, Three-dimensional model for capillary nanobridges and capillary forces, Modelling Simul. Mater. Sci. Eng. 15, 305–317.

[21] Jung, Y.C. and Bhushan, B., 2006, Contact angle, adhesion and friction properties of micro- and nanopatterned polymers for super hydrophobicity, Nanotechnology, 17, 4970–4980.

[22] Wei, Z. and Zhao, Y., 2007, Growth of liquid bridge in AFM, J. Phys. D: Appl. Phys., 40, 4368–4375.

[23] Liu, B., Sheng, G. and Lim, S.T., 1997, Meniscus force modelling and study on the fluctuation of stiction/friction force in CSS test process, IEEE Transactions on Magnetics, 33, 3121–3123.

[24] Jinesh, K.B. and Frenken, J.W. M., 2006, Capillary condensation in atomic scale friction: How water acts like a glue?, Physical Review Letters, 96, 166103.

[25] Higgins, D.D., Marmo, B.A., Jeffree, C.E., Koutsos, V. and Blackford, J.R., 2008, Morphology of ice wear from rubber–ice friction tests and its dependence on temperature and sliding velocity, Wear, 265, 634–644.

[26] Buhl, D., Fauve, M. and Rhyner, H., 2001, The kinetic friction of polyethylene on snow: the influence of the snow temperature and the load, Cold Regions Science and Technology, 33, 133-140.

[27] Maeno N. and Arakawa M., 2004, Adhesion shear theory of ice friction at low sliding velocities, combined with ice sintering, Journal of applied Physics, 95 (1) 134-139.

[28] Bäurle, L., Kaempfer, U., Szabó, D. and Spencer, N.D., 2007, Sliding friction of polyethylene on snow and ice: Contact area and modeling, Cold Regions Science and Technology 47, 276–289.

[29] Bowden, F.P., 1953, Friction on snow and ice, Proceedings of the Royal Society of London. Series A, Mathematical and Physical Sciences, 217, 462-478.

[30] Slotfeldt-Ellingsen, D. and Torgersenf, L., 1983, Water in ice: influence on friction? J. Phys. D: Appl. Phys., 16, 1715-1719.

[31] Baurlea, L., Szabo, D., Fauvea, M., Rhyner H. and Spencer N.D., 2006, Sliding friction of polyethylene on ice: tribometer measurements, Tribology Letters, 24, 77-84.

[32] Liferova, P. and Bonnemaire, B., 2005, Ice rubble behaviour and strength: Part I. Review of testing and interpretation of results, Cold Regions Science and Technology, 41,135–151.

[33] Shafrova, S. and Høyland, K.V., 2008, The freeze-bond strength in first-year ice ridges. Small-scale field and laboratory experiments, Cold Regions Science and Technology 54, 54–71.

[34] Frederking, R.M.W. and Timco, G.W., 1984, Measurement of shear strength of granular discontinuous columnar sea ice, Cold Regions Science and Technology 9, 215–220.

[35] Timco, G.W. and Weeks, W.F., 2009, A review of the engineering properties of sea ice, Cold Regions Science and Technology, in press.

[36] Abrate, S., 1992, Vibrations of belts and belt drives, Mech. Mach. Theory, 27, 6, 645.

[37] Beikmann, R.S., Perkins, N.C. and Ulsoy, A.G., 1997, Design and analysis of automotive serpentine belt drive systems for steady state performance, Transaction of the ASME, Journal of Mechanical Design, 119, 162.

[38] Connell, J.E. and Meckstroth, R.J., 1994, Influence of Pulley Profile on Automotive Accessory Drive Noise, SAE Paper 940688.

[39] Sheng, G., Liu, K., Otremba, J., Pang, J. and Qatu, M., 2006, A new mechanism of belt slip dynamic instability and noise in automotive accessory belt drive systems, Int. J. Vehicle Noise and Vibration, 2, 4.